CHEMICAL ENGINEERING SCIENCE
GENIE CHIMIQUE

VOL. 6 1957 No. 6

VOL. 6 956/57

The effect of absorption on the wetted area of absorption towers

J. Bond and M. B. Donald

Department of Chemical Engineering, University College, London

(*Received* 3 *January* 1957)

Abstract—The change in the wetted area of a packing when absorbing in water a gas having a high latent heat of solution has been noted in the literature. No explanation for this phenomenon has previously been given. Experiments have been carried out using a 1 in. diameter wetted wall column for absorbing ammonia from a gas stream and the water rate which will just maintain a continouous film on the column has been found. Below this water rate the film breaks down and there is a considerable reduction in the area exposed for absorption. Similar results have been obtained by condensing water from a hot saturated air stream on to a water film.

The results are expressed as a difference in the surface tension, at the point where the film breaks, between the main bulk of the liquid and a film of liquid which has become in equilibrium with the main gas stream. The reduction in the surface tension of the liquid due to the absorption of ammonia as well as the heat of solution or condensation of the gas or vapour being absorbed is taken into account and also the opposite effect of the heat of vaporisation when absorbing in hot water.

Ripples on the water film appear to play an important part. The use of a surface active agent like *Teepol* suppresses the ripples and prevents the breakdown of the water film until an extremely low water rate is reached. The breakdown of the film is also found on carbon grid packings and the wetted area has been measured for various flow rates.

The surface tension of ammonia solutions at various temperatures and concentrations were measured and used to correlate the results obtained.

Résumé—La littérature mentionne un changement dans la surface humide du garnissage quand on absorbe dans l'eau un gaz ayant une chaleur latente de dissolution élevée. On n'a pas donné jusqu'ici d'explication de ce phénomène. Les auteurs ont réalisé des expériences avec une colonne à paroi humide de 1 in. de diam., pour l'absorption de l'NH_3 dans un courant gazeux, et ont ainsi trouvé la vitesse de l'eau qui permet d'avoir un film continu dans la colonne. Pour une vitesse inférieure le film se désagrège, et il en résulte une réduction considérable de la surface d'absorption. Des résultats analogues ont été obtenus en condensant l'eau d'un courant d'air saturé chaud sur film d'eau.

Les résultats sont exprimés sous forme d'une différence dans la tension de surface, au point où le film se désagrège ; différence entre la tension du corps principal du liquide et la tension du film de liquide qui est en équilibre avec la masse gazeuse. Il est tenu compte de la réduction dans la tension de surface du liquide ; réduction due à l'absorption de l'ammoniac aussi bien qu'à la chaleur de dissolution ou de condensation du gaz ou de la vapeur absorbés.

Il est également tenu compte de l'effet opposé dû à la chaleur de vaporisation quand on absorbe dans l'eau chaude.

Il semble que les rides à la surface de l'eau jouent un rôle important. L'utilisation d'un agent tensio-actif tel que le teepol supprime les rides, évite la désagrégation du film jusqu'à de très faibles débits. La brisure du film se produit également sur des garnissages du type grille de carbone et la surface humide a été mesurée pour différentes vitesses d'écoulement.

Les auteurs ont mesuré la tension de surface de solutions d'ammoniac à différentes températures et concentrations, ce qui a permis de coordonner les résultats obtenus.

Introduction

Much of the design and experimental work on absorption is based on an assumed value of the wetted area of the packing. In the standard formula for expressing the mass transfer coefficient in terms of the Schmidt Number, gas and liquid rates, the value of the exponent of the liquid rate varies very considerably with the liquid rates used and with the gas being absorbed. Pratt [8] gives an indication of the effect of absorption on the wetted area of a packing by giving different Minimum Equivalent Liquor Rates for various absorption systems. An example is also given of the effect of ammonia absorption on the water film on a wetted wall column which is found to break down prematurely. This he ascribes to the latent heat of solution of the ammonia but no further explanation is given.

Other workers have noted that the packing of a tower has not been completely wetted during an absorption process. Molstad and Parsly [7] found that the wetted area of a packed tower varied from 10–20% to 80–90% when absorbing ethanol vapour in water at various water rates. They found the value of $K_G a$ depended on the water rate to a greater extent than was expected. Chilton, Duffey and Vernon [1] found inconsistent results in ammonia absorption as a result of channelling of the liquid even though they had good initial liquid distribution. Kowalke, Hougen and Watson [5] reported the altering of the effective distribution of the water in a packed tower when absorbing ammonia from air. Many other workers have found inconsistent results when absorbing a highly soluble gas and have concluded that there is a change in the interfacial area.

The first direct measurment of the wetted area of a packing was carried out by Mayo, Hunter and Nash [6] using an air and water system but with no absorption taking place. Similar results were obtained by Grimley [3] using an air and water system. Weisman and Bonilla [11] and Shulman and De Gouff [9] also used an air and water system but obtained conflicting results by different methods. More recently Shulman, Ullrich, Proulx and Zimmerman [10] measured the mass transfer coefficient and the wetted area of naphthalene Raschig rings and Beryl saddles. From a correlation of j_D and a modified Reynolds number for the gas rate, the mass transfer coefficient (k_G) for ammonia absorption was calculated and compared with the value of $k_G a$ obtained by Fellinger [2]. In this way the effective interfacial area (a) was determined for ammonia absorption and it was found that it varied considerably with the water rate.

Although it has been recognised for some time that the wetted area of a packing can be modified during an absorption process, little work on this phenomenon has been published. This investigation was carried out to try to explain this phenomenon.

Apparatus and Procedure

Before the results obtained could be correlated on the basis of a surface tension difference, the surface tension of ammonia solutions in softened water was determined for concentrations between 0 and 13 g/l. and temperatures between 20 and 50°C. As expected the surface tension decreased with the increase in ammonia concentration. Jaeger's Maximum Bubble Pressure method was used for the determinations. Softened water was used in the column to avoid the deposition of salts on the glass surface. Distilled water would have been preferable but the quantities required would be considerable.

The initial absorption experiments were carried out in a 1 in. diameter and 4 ft long wetted wall column. To obtain reproducable results, great care was taken to line up the column vertically in order to get even distribution of the water on the top of the column. With no absorption taking place, a continuous film of water was maintained at water rates down to 0·05 c.c./sec cm.

The gas was sampled at the inlet and outlet of the column by drawing a known volume of gas through N sulphuric acid. The solution was back titrated to determine the concentration of ammonia in the gas stream. A similar method was used for determining the concentration of the ammonia in the water leaving the column. The temperature of the gas and water entering and leaving the column and the humidity of the air entering the column were taken. Flow measurements were made by calibrated orifice meters.

The hot saturated air used in one series of experiments was obtained by mixing steam and air before entering the column. Some steam was allowed to condense out before entering the column to ensure complete humidification of the air. Provision was also made for heating the water and air supplied to the column.

The column was cleaned with dilute nitric acid; then washed with water before the start of each experiment. A high flow rate of softened water was then passed down

VOL 6 1956

the column and the air and ammonia (or steam) flows adjusted to the required amounts. The water rate was reduced slowly and the condition of the film viewed through the glass wall. The point at which the film started to break at the base of the column was readily seen. If the water rate was reduced still further, the whole of the film on the column was broken and the water ran down one side in an irregular manner. The rest of the column was left dry. To reform the film, the water rate had to be increased considerably before a continuous film was formed. By careful adjustment of the water rate, the breakdown of the film could be controlled so that it just started at the base of the column. Occasionally the small area of column which had become dry, was rewetted but soon another dry patch formed at the column base. It was at this minimum water rate when the film had just started to break at the bottom of the column that the experiments were carried out and the results obtained. In all the experiments this minimum water rate was above that water rate which would maintain a continuous film on the column when no absorption was taking place.

VOL. 6 956/57

Results

The breakdown of the film on the column was initially a breaking of the surface of the film and consequently the surface tension between the gas and the liquid must play an important part. The first method of correlating the results was based on the change in the surface tension as the water moved down the column. From the mass transfer coefficients and the surface tension results, the change in surface tension per unit height could be calculated for the base of the column where the film initially started to break. This, however, did not give any indication of the mechanism of the breakdown of the film. The second method, which is given here, was based on the difference in surface tension between adjacent parts of the film at the base of the column. Just prior to the film breaking, a thin film was present on the column wall; this film then disappeared into the main portion of the water as a result of its lower surface tension. A dry patch was then formed on the column and an increase in the water rate was required to reform the film. Now the maximum temperature and concentration that the thin film can reach is when it is in equilibrium with the gas stream. The difference in surface tension at the base of the column between the bulk of the liquid and the thin (or equilibrium) film was used to correlate these results. The surface tension of the liquid at the bottom of the column was found from the analysis of the effluent. The actual surface concentration and temperature will be slightly higher than those used but they cannot be readily determined. The temperature and concentration of the equilibrium film was obtained from the inlet gas conditions and a plot similar to Fig. 1 was obtained for each experiment. This

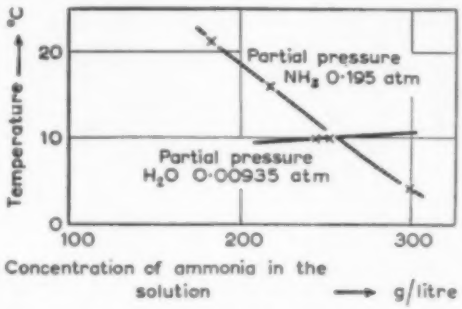

Fig. 1. Equilibrium film conditions at base of column.

was constructed by plotting the concentration of ammonia solutions at various temperatures which had a partial pressure of ammonia equal to the inlet gas concentration. Another line was obtained for solutions having a partial pressure of water vapour equal to that in the inlet gas. The intersection of the two lines gave the temperature and ammonia concentration of the solution which was in equilibrium with the inlet gas to the column. The temperature of the equilibrium film was generally about 10°C and had a high ammonia concentration. At these concentrations and temperatures there is very little alteration in the surface tension with small temperature changes, and hence the surface tension values used are taken from the International Critical Tables.

Concentration of ammonia varied

The first experiments were carried out at room temperature using 5–50% ammonia in the gas stream and total gas velocities of 91·5 cm/sec, 152·0 cm/sec, and 244·0 cm/sec. The water rate at which the film just started to break was plotted against the surface tension difference as shown in Fig. 2. In these experiments no account was taken of the effect of evaporation of the water into the

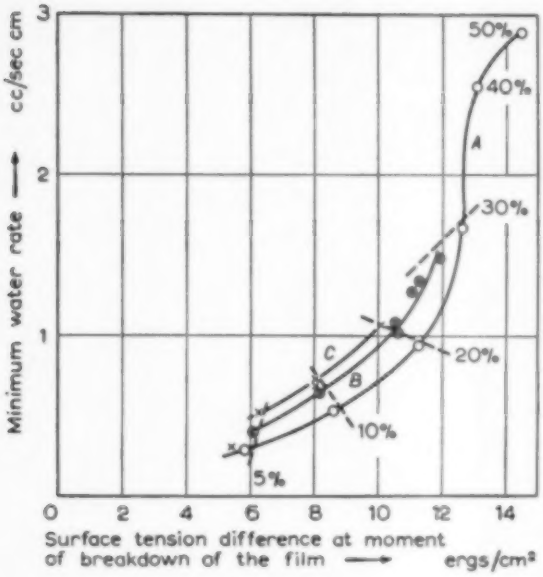

Fig. 2. Absorption of ammonia.
A – Inlet gas velocity 91·5 cm/sec
B – Inlet gas velocity 152·0 cm/sec
C – Inlet gas velocity 244·0 cm/sec
Inlet concentration of ammonia in air in percentage is shown by dotted line.

gas stream as this only reduced the temperature of the water by a small amount. For a given gas velocity, higher water rates were required to maintain the film on the column as the ammonia gas concentration in the air was increased.

Temperature and concentration varied

In the second series of experiments, the temperature of the incoming water was raised successively from 25°C to 70°C so that there was considerable evaporation to counter the effect of the heat of solution of the ammonia. Fig. 3 shows the resultant heating or cooling of the water at the base of the column, calculated from the mass transfer coefficients, latent heats of solution and evaporation against the minimum water rate. Separate lines were obtained for each ammonia gas inlet concentration. As the inlet water temperature was raised, the heat lost by evaporation increased and reduced the effect of the heat of solution of the ammonia with a resultant drop in the minimum water rate. Eventually the heat

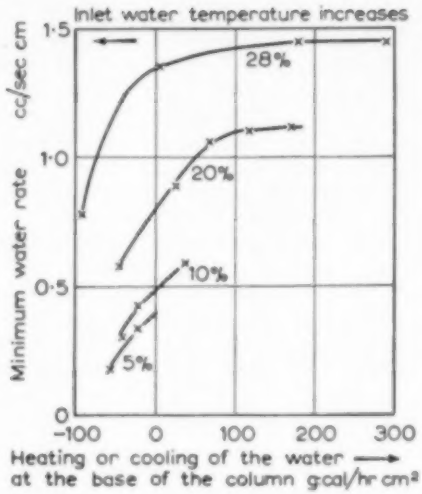
Inlet water temperature increases
Minimum water rate cc/sec cm
Heating or cooling of the water ⟶ at the base of the column g-cal/hr cm²
28%
20%
10%
5%

Fig. 3. Heating or cooling effect on the minimum water rate for various inlet ammonia concentrations in air (%). See Table 1 for inlet and outlet water temperatures.

lost by evaporation exceeded the heat gained by absorption of the ammonia. However, the water film was still liable to break down due to the effect of the ammonia concentration on the surface tension. Fig. 4 gives these results plotted

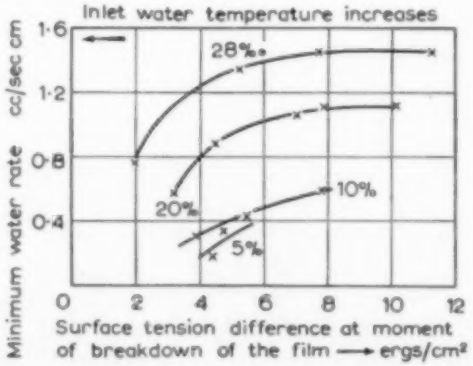

Fig. 4. Absorption of ammonia in hot water (25–70°C). Inlet ammonia concentration given in percentage. Total gas velocity 152·0 cm/sec. See Table 1 for inlet and outlet water temperatures.

on the basis of the surface tension difference between the main film and the equilibrium film. Table 1 gives the inlet and outlet temperature of the gas and water for these results.

Table 1

Ammonia in Inlet Gas %	*Minimum Water Rate c.c./sec cm*	*Inlet Water Temperature °C*	*Outlet Water Temperature °C*	*Heating or cooling of water at base of the column g cal./hr cm²*	*Surface Tension Difference ergs/cm²*
5·35	0·34	39·5	37·3	− 23·9	4·75
4·85	0·186	54·4	36·9	− 57·5	4·40
9·06	0·598	29·5	39·6	+ 36·6	7·80
9·5	0·439	43·0	41·7	− 23·9	5·50
10·5	0·306	49·8	46·9	− 41·6	3·87
19·6	1·120	25·3	29·1	+ 170·0	10·13
20·0	1·110	34·4	37·8	+ 118·0	7·90
19·7	1·060	40·5	43·5	+ 65·6	7·05
19·6	0·891	49·0	49·0	+ 14·2	4·50
20·0	0·585	57·5	55·0	− 44·5	3·20
27·6	1·450	27·6	32·0	+ 289·0	11·28
28·0	1·450	40·9	43·8	+ 178·0	7·78
28·5	1·350	54·8	56·3	+ 4·9	5·25
27·5	0·778	68·6	65·5	− 92·1	2·00

Absorption of water vapour

To show that the concentration effect was not the only factor which affects the breakdown of the film, some experiments were made using an air stream heated to between 48 and 50°C and saturated with water vapour. The humid air stream was cooled by a falling film of water initially at 18°C and water vapour condensed and raised the temperature of the film. In this case there was a heating of the surface but no concentration effect. The film on the column was found to break down in a similar manner as before. The temperature of the equilibrium film was the wet bulb temperature of the gas and from this the surface tension of the equilibrium film was found. The surface tension of the main film was found from the temperature of the water leaving the column. As the difference between the surface tension of the main film and equilibrium film increased, a greater water rate was required to maintain the continuous film on the column. Fig. 5 gives the results obtained but in this case no effect of gas velocity, as in Fig. 2, is is found despite considerable variation.

The addition of a surface active agent (*Teepol*) to the water supplied to the column suppressed the ripples and no breakdown of the film was observed until a very low water rate was reached (0·23 cm/sec cm) in both the ammonia and water vapour absorption experiments. This low water rate was independent of the gas in the column. Furthermore, no breakdown of the film was observed when evaporating water from a falling film.

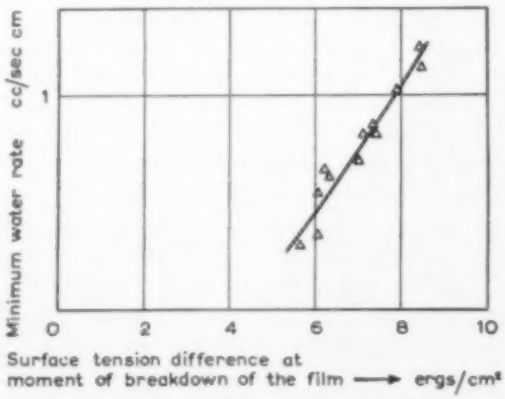

Fig. 5. Absorption of water vapour in cold water.

Absorption on serrated carbon grids

Some experiments were also carried out to determine the wetted area of an industrial type of packing for various gas concentrations using 1 in. carbon grid, $\frac{1}{8}$ in. thick and $3\frac{3}{8}$ in. wide, marked out in squares.

An even distribution of water was maintained to the grid and at various gas and water rates the area wetted by the water was noted. With no absorption the grid was completely wetted at a water rate of 0·2 c.c./sec. The results are shown in Fig. 6. No change in wetted area was found with varying velocities but this may have been due to the low velocities used (13·2 cm/sec maximum). In these results it was particularly noticeable that the water flowed over the grid in a parabolic manner.

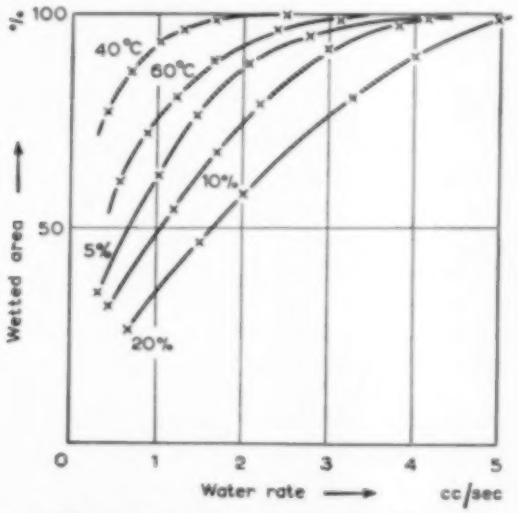

Fig. 6. Wetting of a carbon grid while absorbing ammonia or water vapour. Ammonia concentration in air in %. Inlet saturated air temperature in °C.

The water fell from the drip point of the grid on to the top of the grid below and the majority of the water spilt over on to its face. The main film thus started from a point source and spread out giving a parabolic pattern. The remaining water ran along the top of the grid and overflowed on to the face. This secondary water formed a small thin film between the parabolic films beneath the drip points. The parabolic film was comparatively thick compared with the thin film between but it was the latter film which broke first and formed a dry patch when absorption was taking place. In some cases, particularly at the higher ammonia gas concentrations, the main parabolic film also broke down when absorption was taking place.

Discussion of Results

The presence of ripples appear to play an important part in the breaking down of the film. When the ripples are suppressed by a surface active agent, the film does not break down while absorbing ammonia or water vapour until a very low water rate is reached. This low water rate is independent of the absorption of the ammonia or water vapour.

Grimley [3] found that ripples start at a Reynolds Number of 25, reach a maximum of intensity at 800 and cease at a Reynolds Number of about 1,000, after which turbulence appears to set in. Plotting the results using the Reynolds Number for the minimum water rate, Fig. 7 is obtained. The gradient of curve *B* decreases as the water rate approaches a Reynolds Number of 1,000. Curves *C* and *D* follow a similar line

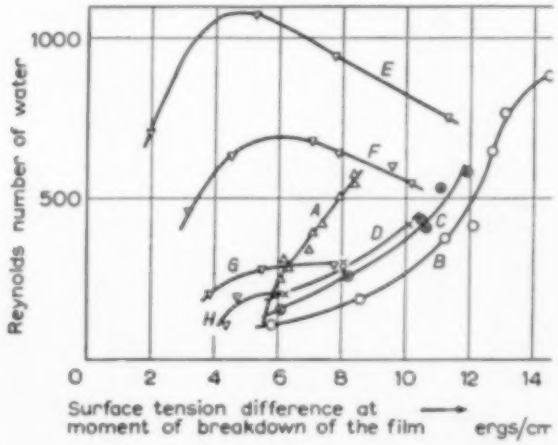

Fig. 7.

A – Absorption of water vapour
B – ,, ,, ammonia at 91·5 cm/sec in water
C – ,, ,, ,, ,, 152·0 cm/sec ,, ,,
D – ,, ,, ,, ,, 244·0 cm/sec ,, ,,
E – ,, ,, 30% ammonia in hot water (25 – 70°C)
F – ,, ,, 20% ,, ,, ,, ,,
G – ,, ,, 10% ,, ,, ,, ,,
H – ,, ,, 5% ,, ,, ,, ,,

VOL.
6
1956/57

but it was not possible to reach the higher Reynolds Number in the experiments. Curve *E* reaches a maximum at a Reynolds Number of 1,080. At the higher water rates it was often found that the dry patch formed at the base of the column was rewetted, only to be followed by another dry patch. At high water rates the turbulence in the water film appeared to reduce the effect of the ripples and rewet the column whenever a dry patch was formed.

The presence of ripples on the column gives rise to an unevenness in the film. In the case of ammonia absorption, the ammonia diffuses through the air to the surface of the water and dissolves but the diffusion in the water layer is greater where there is a thick film at the crest of a ripple and hence larger volume of water, than at the trough where the film is thin. The trough will then have a higher concentration of ammonia than the crest and the maximum concentration it can reach is when it is in equilibrium with the gas stream. The temperature of the trough will also be determined by the equilibrium conditions. As a result of the equilibrium conditions for the trough, the surface tension will be lower than that of the crest or thick film. This difference is sufficient to draw the thin film into the thick film leaving a dry patch on the bottom of the column. An increase in the water rate is then required to rewet the dry part of the column.

As the temperature of the inlet water is increased during ammonia absorption, the evaporation of the water begins to play an important role and is a counter-effect to the heat of solution. The equilibrium film remains at substantially the same temperature and concentration for a given inlet gas concentration as the inlet water temperature is increased. The temperature of the main bulk of the liquid at the bottom of the column will depend on the amount of absorption and evaporation that is taking place. At low inlet water temperatures there is a resultant heating of the liquid but, as the inlet water temperature is increased, more water is vaporised and less ammonia is absorbed. At the highest inlet water temperature used the heat of vaporisation is greater than the heat of solution of the ammonia and the outlet temperature of the liquid is reduced. The surface tension of the main bulk of the liquid at the base of the column is affected by the temperature as well as the ammonia concentration, the net result being a decrease as the inlet water temperature is increased. Since the surface tension of the equilibrium film is substantially constant then the surface tension difference at the base of the column is decreased and a lower minimum wetting rate is required for the column. Even though the heat lost by evaporation can exceed the heat gained by the heat of solution of ammonia the film on the column can still break down owing to the concentration effect, the surface tension of the bulk of the liquid being slightly higher than the surface tension of the equilibrium film.

The low water rate at which KANTYKA and HINCKLIEFF [4] were able to operate their adiabatic hydrogen chloride absorber was probably due to the large amount of evaporation of water that was taking place. The heat lost by evaporation counteracted the heat gained by the solution of hydrogen chloride with the effect that the surface tension difference was reduced. A much lower water rate than normally used in hydrogen chloride absorption was possible while still maintaining efficient wetting of the packing.

In the case of the condensation of water vapour on the falling film, there was no concentration effect. However, the thin film in equilibrium with the gas stream would have the same temperature as the gas stream. The main part of the film would have a lower temperature than the humid gas stream and hence a higher surface tension than the equilibrium film. The surface tension difference was sufficient to form a dry patch on the column.

When there is evaporation from the water film into an inert gas stream, no premature breakdown of the film is observed.

In the case of carbon grids, the break comes first between the parabolic water films below the drip points but at high ammonia gas concentrations the main parabolic films often break down. No effect of the velocity of the gas was found in this case but it was probably due to the very low values obtainable. Alternatively, it may be

due to the different flow patterns obtained on the grids where thick and thin films are much more pronounced compared with wetted wall columns.

Conclusions

(1) The absorption of ammonia or water vapour on a continuous film of water with a rippled surface can result in its premature breakdown and hence reduce the efficiency of the column.

(2) The breakdown can be effected by concentration as well as temperature effects.

(3) An increase in the water temperature will increase the heat lost by evaporation. This will counteract the heat gained by absorption and hence reduce the water rate at which the film breaks.

(4) The breakdown of the film can be prevented by using a surface active agent.

Acknowledgements—The help provided by the Trustees of the Leverhulme Trust in the provision of a grant to cover this work, originally published for a Ph.D. degree of London University, and the helpful suggestions of Dr. W. S. Norman are gratefully acknowledged.

References

[1] Chilton T. H., Duffey H. R., and Vernon H. C. *Ind. Engng. Chem.* 1937 **29** 298.

[2] Fellinger L. Sc.D. Thesis, Mass. Inst. Technol 1941.

[3] Grimly S. S. Ph.D. Thesis, London University 1947.

[4] Kantyka T. A. and Hincklieff H. R. *Trans. Instn. Chem. Engrs., Lond.* 1954 **32** 236.

[5] Kowalke O. L., Hougen O. A., and Watson K. M. *Chem. Metall. Engng.*, 1925 **32** 506.

[6] Mayo F., Hunter T. G., and Nash A. W. *J. Soc. Chem. Ind.* 1935 **54** 375 T.

[7] Molstad M. C. and Parsly L. F. *Chem. Prog. Engng.* 1950 **46** 20.

[8] Pratt H. R. C. *Trans. Instn. Chem. Engrs.* 1951 **29** 195.

[9] Shulman H. L. and De Gouff J. J. *Ind. Engng. Chem.* 1952 **44** 1915.

[10] Shulman H. L., Ullrick C. F., Proulx A. Z. and Zimmerman J. O. *J. Amer. Inst. Chem. Engng.* 1955 **1** 253.

[11] Weisman J. and Bonilla C. F. *Ind. Engng. Chem.* 1950 **42** 1099.

Chemical Engineering Science, 1957, Vol. 6, pp. 245 to 261. Pergamon Press Ltd.

The quaternary system: benzene—carbon tetrachloride—acetic acid—water at 25°C

R. G. H. PRINCE* and T. G. HUNTER

Chemical Engineering Department, University of Sydney, N.S.W., Australia

(*Received* 20 *May* 1956; *shortened version* 30 *January* 1957)

Abstract—Apparatus is described for the accurate determination of liquid – liquid equilibrium in ternary and quaternary systems by the synthetic method; and in particular, a microburette for use in cloud point titrations, and a flask which enables the weights of the equilibrium phases to be determined directly. Tie lines may then be located by the "lever rule," more accurately and conveniently than in the method of OTHMER, WHITE and TRUEGER [14]. Results are presented for the system benzene – carbon tetrachloride – acetic acid – water at 25°C, and relationships between the equilibrium concentrations in the quaternary and the ternary systems are discussed.

Résumé—Les auteurs décrivent un appareillage pour la détermination précise de l'équilibre liquide-liquide dans les systèmes ternaires et quaternaires par la méthode synthétique. Ils décrivent en particulier une microburette utilisable dans les titrages en point de trouble et un flacon qui permet de déterminer directement les poids des phases en équilibre. Les lignes de raccordement peuvent être alors déterminées par l'utilisation de la "courbe de distribution" plus pratique et plus adéquate que dans la méthode d'OTHMER, WHITE, et TRUEGER. Les auteurs donnent des résultats pour le système benzène – tétrachlorure de carbone – acide acétique – eau à 25°C et discutent les relations entre les concentrations d'équilibre dans les systèmes ternaires et quaternaires.

INTRODUCTION

EQUILIBRIUM relationships in four component two phase liquid systems are required in the design of solvent extraction processes involving complex solvents. As it is not often possible to calculate such equilibria theoretically, and practical determinations are difficult and tedious, a first step is to relate the equilibrium concentrations in the quaternary systems to those in the component ternaries, about which more is generally known, or which may be determined comparatively easily. Quaternary systems have been studied for this purpose by BRANCKER, HUNTER and NASH [4] and, more recently, by CHANG and MOULTON [7]. The former postulated a comprehensive set of relations between the quaternary and ternary equilibrium concentrations, which will be discussed below. These relations were applicable to the type of quaternary system illustrated in Fig. 1 (a), in which one pair of components is partially miscible.

CHANG and MOULTON in their study of several quaternary systems of the type illustrated in Fig. 1 (b), where one component is partially miscible with two others, found a relationship

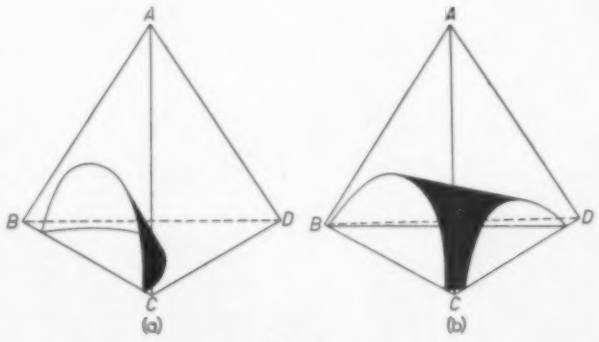

FIG. 1.

*Present address: The Distillers Co. Ltd., Research and Development Department, Great Burgh, Epsom, Surrey.

between the quaternary equilibrium concentrations and one of the ternary systems, viz. the double non-consolute pair ternary *BCD* of Fig. 1 (b). It was decided to investigate a number of quaternary systems in order to examine further the existence of such relations. The apparatus and experimental techniques evolved for this purpose, and the results obtained for a quaternary system of the type shown in Fig. 1 (b), namely benzene – carbon tetrachloride – acetic acid – water, are presented here.

Experimental Methods

The apparatus and techniques employed will be described briefly, as they are novel in some respects, and appear to have advantages over the more traditional methods. It was necessary that methods be selected which could be used with the widest possible range of systems, and that they be sufficiently accurate to discriminate between competing correlations (this point has been discussed in detail by Hand [9]).

The first of these criteria eliminated direct analysis of the equilibrium phases, and the alternative " synthetic " method was adopted. This two step method requires (i) the determination of the saturation isotherm by titration, and (ii) the location of tie lines, using information obtained in (i) to identify the tie line compositions. The usual method of tie line location involves in an n component system analysis of the phases for n-2 components, or measurement of n-2 physical properties.

A more elegant method of tie line location is based on the " lever rule," which states that the point representing the initial mixture lies on a line joining the points representing the compositions of the two equilibrium phases, and divides this line in the inverse ratio of the weights of the two phases. If the initial mixture composition is known, measurement of this ratio is then sufficient to determine the tie line in a ternary system provided the saturation curve is available. This method was applied in early work [3, 11], but in both cases invalidating assumptions were made. Valid determinations of ternary tie lines were made by Othmer, White and Trueger [14]; they made up mixtures in a graduated cylinder, so that, after attaining equilibrium and allowing the phases to settle, phase volumes could be read off. Density measurements were required to convert the volumes to weights. A graphical method for locating tie lines from such data was given later [13].

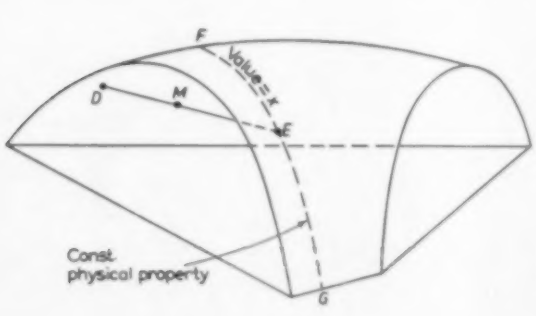

Fig. 2.

This method when applied to a quaternary system requires one additional measurement, which can conveniently be a physical property of one of the saturated phases. In Fig. 2 the saturation frustrum of the quaternary system type illustrated in Fig. 1 (b) has been reproduced. *DE* is a quaternary tie line which passes through the overall or initial mixture composition point *M*; and points *D* and *E* lying on the saturation surface of the frustrum represent compositions of quaternary phases in equilibrium. A convenient physical property of the phase *E* has been ascertained to be of value x. The weight of the two phases *D* and *E* has been determined, while the overall mixture composition *M* is also known. The point *E* must lie on the line *FG* of constant physical property (value x), which line lies on the saturation surface and has been obtained in the course of determining that surface. Further, the quaternary tie line *DE* must be so located in space that the ratio DM/ME equals the ratio (weight of phase *E*)/(weight of phase *D*), and it may then be found by trial and error. This procedure was used in the present work. The method differed in practice from Othmer's in that the phases were separated and weighed directly, rather than that the weights were inferred from phase volume and density determinations.

Apparatus

In the cloud point titrations (by which the saturation isotherm was established) and the tie line determinations agitation of the solutions was provided by a shaker mechanism which rocked the solution flask through an arc of 10° at speeds which were continuously variable from 90 to 900 oscillations per minute.

The number of points to be determined in the cloud point titrations limited the quantities for each point to such that final volumes of about 20 ml would be obtained. It was then desirable to add titrant in increments of less than 0·002 ml, and hence a microburette was required. Although a large number of designs of such instruments have been published (reviewed by Kirk [10]), none appeared to be completely satisfactory for the present purpose. After extensive trials of several types, the burette shown in Fig. 3 was constructed.

VOL. 6 956/57

This consisted of a stainless steel reservoir, a glass vessel containing the titrant liquid, and a flexible connecting unit, to convey the titrant from the stationary burette to the shaking flask. The dimensions of the reservoir gave a convenient displacement, 8·5 ml. A rubber " piston ring," as illustrated, was found necessary to prevent mercury leakage. 24 BG stainless steel tubing was used for the connecting unit, and fused directly into 1 mm Pyrex capillary tubing. In operation the burette was filled with sufficient clean mercury to cover the glass-metal joint, ensuring that the titrant was kept to the titrant vessel and the connecting unit, and hence only these needed thorough cleaning when changing titrant. After filling the burette with titrant the tip of the steel tube was arranged to be within a half inch of the solution surface, so that during shaking titrant was washed off the tube tip, and hence could be added in increments well below the desired figure.

The burette gave easy and positive control of the rate of titration, and could be mounted conveniently on the thermostat tank. The titrant was protected from atmospheric dirt and moisture, and from evaporation, and had no tendency to leak into the solution to be titrated. Construction in three separate parts made for easy cleaning and filling.

The solution to be titrated was contained in the special stoppered flask, also illustrated in Fig. 3, in which a volume of 20-25 ml of liquid could be safely shaken at speeds of up to 900 oscillations per minute without loss of liquid. For filling and cleaning the stopper was removed, but during titration only the cap on the stopper capillary tube was removed and the steel tube of the microburette inserted through the capillary tubing. Even during a lengthy titration there was little danger of incurring significant losses due to evaporation.

The apparatus used for the location of tie lines is shown in Fig. 4. The bulb was intended to contain about 40 ml of liquid, and had a total volume of about 100 ml. It was filled through the bent neck, which prevented any loss of liquid due to splashing onto ground surfaces. The diameter of the capillary tube was found to be critical, too small a diameter causing excessive rise of liquid, and hence loss, while too large a diameter made phase separation difficult or impossible, due to the formation of bubbles of one phase in the tube. The optimum diameter was found to depend on the surface tensions of the solutions, and that shown (1 mm) was found satisfactory for the system studied, but more recent work with this apparatus on a non-aqueous system required smaller diameter tubing. The bore of the capillary should also be

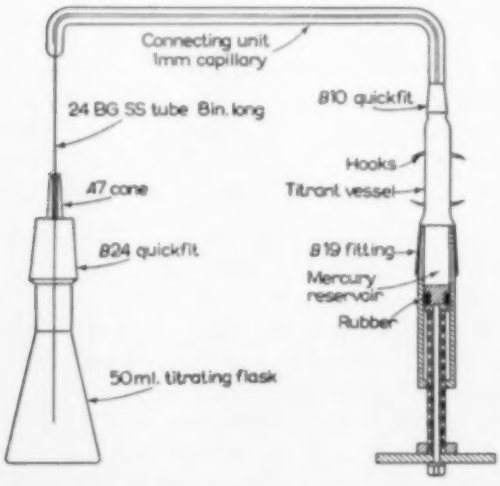

Fig. 3. Titration assembly.

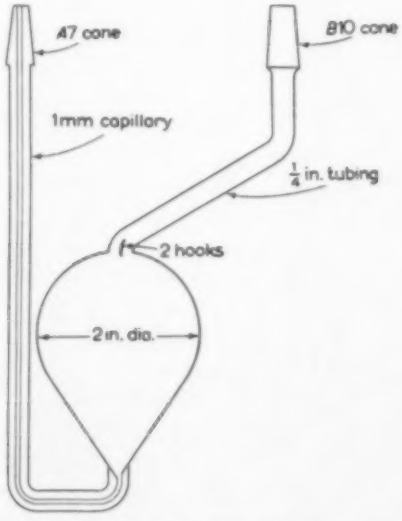

Fig. 4. Equilibrium flask.

uniform so that small quantities of a phase may be estimated. Both neck and capillary tubes were normally closed by mating ground caps.

In making a particular determination, the requisite quantities of components were weighed into the vessel, which was then placed in the thermostat and shaken at about 700 oscillations per minute. Shaking was stopped at frequent intervals, the phases allowed to settle out, and liquid displaced from the capillary tube by applying pressure from a dry air supply, so as to bring this liquid to equilibrium with the bulk of the solution. As this process produced marked turbidity until equilibrium was established, this event could be confirmed visually. After an hour the shaker speed was reduced to 150 oscillations per minute, producing gentle agitation. This enabled the phases to settle, while changing the interface, and helped to remove bubbles of the lower phase remaining in the upper surface of the upper phase. Any such bubbles still remaining could usually be removed by gentle twirling of the vessel after the bulk of the lower phase has been separated. Shaking at the lower speed continued for at least two hours, and was followed by settling for at least one hour. The lower phase was then sampled, if required, by pushing liquid out through the capillary tube by applying air pressure to the neck, followed by removal of the bulk of the lower phase in the same way. The last portions of the lower phase were removed by holding a folded piece of filter paper over the end of the capillary, and in this way a neat separation of the phases could be attained. The vessel was weighed after phase separation, giving the weights of the upper and lower phases.

Densities were determined using 10 ml Sprengel – Ostwald type pycnometers. Samples were pushed into them from the titration or equilibrium flasks through special sampling tubes, which prevented the samples from coming into contact with the outside atmosphere.

All weights were determined to within $\pm$ 0·0001 g. Flasks and pycnometers were weighed against tares, and in all cases the usual precautions were taken to ensure that glassware which was wetted during an experiment would have a reproducible film of moisture on it.

The cloud point titrations and phase separations were carried out in a water thermostat controlled to 25·00 $\pm$ 0·02°C at all points. Three sides of the thermostat were made of plate glass to permit illumination and observation of the solutions.

Materials

Water was redistilled from laboratory distilled water, to which alkaline potassium permanganate had been added, in an all Pyrex apparatus of the type standard for conductivity water, using an entrainment trap [15], the middle third of any batch being collected. The product was stored protected from atmospheric carbon dioxide by self indicating soda asbestos.

Properties: Conductivity: $0{\cdot}73 \times 10^{-6}$ mho/cm at 25·00°C.

Acetic Acid, A.R. quality, was dried by partial freezing until the freezing point exceeded 16°C. A.R. acetic anhydride was added, 20% in excess of that required to convert the water content (calculated from the depression of the freezing point) to acetic acid, and the acid allowed to stand for some days before fractionation in a column packed with 3 mm Fenske helices. After refluxing for 15 hours, 20% of the charge was rejected at a reflux ratio of better than 10 : 1, and 40% collected at a ratio of better than 4 : 1. No rise in boiling point was observed during the collection. Acid was prepared on two occasions, a 2 ft column being used for batch 1 and a 4 ft column for batch 2.

Properties :	Batch 1	Batch 2
B.P. (760 mm.)	117·9	117·9°C
Density, 25°C	1·0438	1·0438g/ml
F.P.	16·52	16·55°C
Water content	0·043	0·028%

Benzene was also prepared in two batches, from thiophene free material. For batch 1 benzene was refluxed and fractionated over sodium in the shorter column, twice recrystallized, and again refluxed and fractionated over sodium, using the same procedure as for the acid. For batch 2 the benzene was washed with chlorsulphonic acid, neutralized and washed with water, refluxed and fractionated over sodium in the 4 ft column, and recrystallized twice.

Properties :	Batch 1	Batch 2
B.P. (760 mm)	80·1	80·1°C
Density, 25°C	0·8732	0·8736 g/ml
F.P.	5·40	5·47°C

Carbon tetrachloride, technical grade, was washed in half gallon lots with 100–200 ml consecutive washes of alcoholic potassium hydroxide, distilled water, sulphuric acid, water, alkaline potassium permanganate, and finally water. The product was allowed to stand over calcium chloride for several days, and was then refluxed and fractionated over dried anhydrous A.R. sodium carbonate, as for the acid.

Properties :

B.P. (760 mm)	76·7°C
Density, 25°C	1·5846 g/ml

The acetic acid, benzene and carbon tetrachloride were stored in storage bottles fitted with delivery burettes, both bottles and burettes being kept under an atmosphere of nitrogen which had been dried over anhydrous magnesium perchlorate, and from which carbon dioxide had been removed by self-indicating soda asbestos.

The Quaternary Isotherm

The quaternary saturation surface was explored by taking sections through the acetic acid and water apices, and finding the saturation curve for each section. Each section could be regarded as a ternary system for this purpose, of components acid, water, and a benzene – carbon tetrachloride mixture. For each section a sufficient quantity of the benzene – carbon tetrachloride mixture was made up by weight, and stored under conditions making a significant change in composition unlikely. The quaternary isotherm was determined as nine such sections, five of these being complete sections of 16 experimental points each, and four sections of eight points only on the water lean side of the isotherm, making 112 experimental points in all. All points were found by cloud point titration, using the apparatus described. For all points in the 8-point sections, and for 12 of the 16 points in each of the complete sections, water was the titrant, as preliminary experiments had shown that where both could be used, titration with water gave better cloud points than titration with the benezene – carbon tetrachloride mixture.

The results are shown in Table 1. In calculating the observed compositions, the water content of the acetic acid and the benzene, found from their freezing points, was taken into account. The specific volumes found for the saturated solutions are also shown. Two series of results are given for the benzene – acetic acid – water ternary, the first being carried out with benzene batch 1, and repeat determinations being made with the purer batch 2, giving the same solubilities as before, within experimental error, but slightly differing specific volumes.

As the solubilities in the various sections are similar, individual results were corrected for over-and under-titration by comparison with the other results, and three charts were made up for the purpose. In the first, the results for the nonaqueous phase with acetic acid concentrations up to 30% were plotted as weight per cent water against weight per cent acid on a scale of 10 cm to 1% water and 1 cm to 1% acid. Results for the aqueous phase were similarly plotted, as benzene + carbon tetrachloride (10 cm to 1%) against acetic acid (0·5 cm to 1%), covering the range to 54% acid. The large changes in composition of all components over the remaining, central range made a similar arithmetic plot unsuitable, and Bancroft's expression for the isotherm [1] was used, log (water/acetic acid) being plotted against log (benzene + carbon tetrachloride)/acetic acid on a 60 cm × 100 cm chart. The necessary binary data were taken from Seidell [20].

For most of the points over-or under-titration had been recorded by noting whether a titrated solution became cloudy after heating to clearness and bringing back to 25°C. Using this information smooth curves were drawn on the above charts to represent the saturation curves of the sections. For points not lying on their appropriate curves, the composition of the "adjusted" saturated solution was calculated from the curve. The "adjusted" values so obtained are given in Table 1. It will be noted that while most of the corrections amount to changes in composition

Table 1. *Cloud point titration results for the quaternary isotherm Benzene (B) – Carbon Tetrachloride (C) – Acetic Acid (A) – Water (W) at* 25°C

		Observed				*Adjusted*				
Point No.	$\frac{C}{B+C}$ *Wt. %*	$B+C$ *Wt. %*	*A Wt. %*	*W Wt. %*	*Specific Volume ml/g at* $\frac{25}{4}$	$B+C$ *Wt. %*	*B Wt. %*	*C Wt. %*	*A Wt. %*	*W Wt. %*
1	0	94·82	4·96	0·22	1·13818	94·86	94·86		4·97	0·17
2	Batch (1)	89·52	10·13	0·35	1·13057	89·54	89·54		10·13	0·33
3	Benzene	82·40	16·93	0·67	1·11878	82·43	82·43		16·93	0·64
4		74·41	24·39	1·19	1·01502	74·39	74·39		24·38	1·22
5		67·83	30·29	1·89	1·09261	67·84	67·84		30·29	1·88
6		59·65	37·26	3·11	1·07612	59·61	59·61		37·25	3·14
7		49·60	45·16	5·24	1·05513	49·60	49·60		45·16	5·24
8		35·87	54·98	9·16	1·02342	35·95	35·95		55·10	8·96
9		26·56	61·05	12·39	1·00263	26·57	26·57		61·08	12·35
10		16·16	65·72	18·11	0·97782	16·13	16·13		65·59	18·27
11		11·61	65·98	22·42	0·96699	11·58	11·58		65·83	22·60
12		4·71	59·51	35·78	0·95359	4·70	4·70		59·45	35·85
13		2·82	53·54	43·64	0·95232	2·84	2·84		53·53	43·63
14		1·57	44·56	53·87	0·95554	1·57	1·57		44·56	53·87
15		0·67	29·70	69·63	0·96703	0·67	0·67		29·70	69·63
16		0·40	14·89	84·72	0·98325	0·40	0·40		14·89	84·72
17	0	94·76	4·90	0·34	1·13773	94·92	94·92		4·91	0·17
18	Batch (2)	89·62	10·03	0·36	1·12974	89·64	89·64		10·03	0·33
19	Benzene	82·24	17·11	0·66	1·11781	82·24	82·24		17·11	0·65
20		75·08	23·81	1·12	1·10544	75·04	75·04		23·80	1·16
21		68·08	30·09	1·83	1·09251	68·07	68·07		30·08	1·85
22		50·06	44·81	5·13	1·05556	50·06	50·06		44·81	5·31
23		36·78	54·33	8·89	1·02550	36·84	36·84		54·46	8·67
24	12·412	94·67	5·11	0·22	1·07723	94·72	82·96	11·76	5·11	0·17
25		89·67	10·01	0·31	1·07268	89·67	78·54	11·13	10·01	0·31
26		82·18	17·18	0·64	1·06542	82·18	71·98	10·20	17·18	0·64
27		74·79	24·03	1·18	1·05740	74·80	65·51	9·28	24·03	1·17
28		67·40	30·67	1·93	1·04817	67·40	59·03	8·37	30·67	1·93
29		59·87	37·05	3·08	1·03771	59·87	52·44	7·43	37·05	3·08
30		49·96	44·85	5·20	1·02331	50·00	43·79	6·21	44·88	5·13
31		36·58	54·51	8·91	1·00182	36·66	32·11	4·55	54·64	8·70
32	24·953	94·71	5·06	0·22	1·01610	94·77	71·12	23·65	5·06	0·16
33		89·86	9·79	0·34	1·01503	89·90	67·47	22·43	9·80	0·29
34		82·19	17·16	0·64	1·01250	82·21	61·70	20·51	17·16	0·62
35		74·88	23·95	1·17	1·00894	74·90	56·21	18·69	23·95	1·15
36		67·28	30·74	1·98	1·00429	67·31	50·51	16·80	30·76	1·93
37		60·34	36·64	3·02	0·99933	60·35	45·29	15·06	36·65	3·00
38		49·92	44·82	5·27	0·99057	50·03	37·55	12·48	44·91	5·07
39		36·37	54·67	8·96	0·97766	36·48	27·38	9·10	54·83	8·69
40		26·53	61·15	12·32	0·96796	26·56	19·93	6·63	61·23	12·21
41		16·57	65·65	17·78	0·95714	16·57	12·44	4·13	65·65	17·78
42	24·953	11·89	65·99	22·12	0·95214	11·89	8·92	2·97	65·99	22·12

Table 1 (*continued*)

Point No.	$\frac{C}{B+C}$ Wt. %	Observed				Adjusted				
		$B+C$ Wt. %	A Wt. %	W Wt. %	Specific Volume ml/g at $\frac{25}{4}$	$B+C$ Wt. %	B Wt. %	C Wt. %	A Wt. %	W Wt. %
43		4·82	59·71	35·47	0·94785	4·83	3·62	1·21	59·90	35·27
44		2·87	53·46	43·67	0·94885	2·75	2·06	0·69	53·53	43·72
45		1·58	44·61	53·81	0·95392	1·53	1·15	0·38	44·63	53·84
46		0·76	29·84	69·41	0·96637	0·65	0·49	0·16	29·87	69·49
47		0·46	14·69	84·84	0·98335	0·37	0·28	0·09	14·70	84·92
48	37·436	94·79	5·01	0·19	0·95542	94·83	59·33	35·50	5·01	0·15
49		89·84	9·88	0·28	0·95775	89·84	56·21	33·63	9·88	0·28
50		82·45	16·97	0·58	0·95953	82·44	51·58	30·68	16·97	0·59
51		74·91	23·96	1·13	0·96073	74·90	46·86	28·04	23·96	1·14
52		67·44	30·60	1·97	0·96094	67·48	42·22	25·26	30·62	1·91
53		59·84	37·00	3·15	0·96010	59·90	37·48	22·42	37·03	3·06
54		47·39	46·68	5·93	—	47·58	29·78	17·80	46·86	5·56
55		36·34	54·77	8·88	0·95401	36·43	22·79	13·63	54·90	8·66
56	49·965	94·67	5·10	0·22	0·89426	94·75	47·41	47·34	5·10	0·14
57		89·93	9·80	0·27	0·89928	89·93	45·00	44·93	9·80	0·27
58		82·65	16·78	0·57	0·90618	82·66	41·36	41·30	16·78	0·56
59		75·12	23·82	1·07	0·91209	75·09	37·57	37·52	23·81	1·11
60		67·76	30·31	1·93	0·91684	67·80	33·92	33·88	30·33	1·87
61		60·70	36·29	3·01	0·92065	60·76	30·40	30·36	36·35	2·91
62		50·13	44·62	5·25	0·92530	50·26	25·15	25·11	44·74	5·00
63		36·83	54·54	8·62	0·93004	36·89	18·46	18·43	54·63	8·48
64		26·85	61·19	11·96	0·93316	26·85	13·43	13·42	61·19	11·96
65		16·95	65·69	17·37	0·93534	16·95	8·48	8·47	65·69	17·37
66		11·52	66·08	22·40	0·93678	11·52	5·76	5·76	66·08	22·40
67		5·22	60·73	34·05	0·94088	5·23	2·62	2·61	60·81	33·96
68		2·79	53·69	43·52	0·94547	2·79	1·40	1·39	53·69	43·52
69		1·52	44·30	54·18	0·95247	1·46	0·73	0·73	44·33	54·21
70		0·76	29·68	69·56	0·96599	0·62	0·31	0·31	29·72	69·66
71		0·44	14·91	84·65	0·98288	0·35	0·18	0·17	14·92	84·73
72	62·460	94·93	4·96	0·11	0·83354	94·92	35·63	59·29	4·96	0·12
73		89·93	9·92	0·16	0·84169	89·85	33·73	56·12	9·91	0·25
74		82·45	17·00	0·54	0·85320	82·44	30·95	51·49	17·00	0·55
75		74·67	24·20	1·13	0·86433	74·68	28·03	46·65	24·20	1·12
76		67·68	30·39	1·93	0·87319	67·71	25·42	42·29	30·41	1·88
77		59·85	36·97	3·18	0·88215	59·94	22·50	37·44	37·03	3·03
78		49·78	44·92	5·30	0·89285	49·93	18·74	13·19	45·07	5·01
79		36·73	54·75	8·52	0·90612	36·79	13·81	22·98	54·84	8·37
80	75·216	94·87	5·02	0·10	0·77094	94·87	23·51	71·36	5·02	0·10
81		89·98	9·83	0·19	0·78244	89·95	22·29	67·66	9·83	0·22
82		82·51	16·98	0·51	0·79889	82·50	20·45	62·05	16·98	0·52
83	75·216	74·90	24·02	1·08	0·81433	74·91	18·57	56·34	24·02	1·07
84		67·68	30·39	1·92	0·82837	67·71	16·78	50·93	30·41	1·87

VOL. 6 1956/57

Table 1 (*continued*)

Point No.	$\frac{C}{B+C}$ Wt. %	Observed				Adjusted				
		$B+C$ Wt. %	A Wt. %	W Wt. %	Specific Volume ml/g at $\frac{25}{4}$	$B+C$ Wt. %	B Wt. %	C Wt. %	A Wt. %	W Wt. %
85		60·05	36·83	3·12	0·84197	60·10	14·90	45·20	36·86	3·04
86		50·07	44·80	5·13	0·85838	50·20	12·44	37·76	44·92	4·88
87		36·85	54·89	8·27	0·88142	36·88	9·14	27·74	54·93	8·20
88		26·91	61·55	11·53	0·89751	26·91	6·67	20·24	61·55	11·53
89		17·00	66·08	16·91	0·91282	17·00	4·21	12·79	66·08	16·91
90		11·92	66·49	21·59	0·92094	11·92	2·95	8·97	66·49	21·59
91		4·96	60·66	34·38	0·93485	4·96	1·23	3·73	60·66	34·38
92		2·83	54·36	42·81	0·94157	2·87	0·71	2·16	54·34	42·79
93		1·42	44·34	54·24	0·95096	1·42	0·35	1·07	44·34	54·24
94		0·63	29·62	69·75	0·96546	0·60	0·15	0·45	29·63	69·77
95		0·56	14·80	84·64	0·98284	0·32	0·08	0·24	14·83	84·85
96	87·776	95·00	4·94	0·06	0·70938	94·97	11·61	83·36	4·94	0·09
97		89·92	9·92	0·16	0·72440	89·88	10·99	78·89	9·92	0·20
98		83·07	16·49	0·44	0·74372	83·05	10·15	72·90	16·49	0·46
99		74·97	23·98	1·05	0·76546	74·98	9·17	65·81	23·98	1·04
100		67·60	30·51	1·90	0·78441	67·61	8·26	59·35	30·52	1·88
101		59·98	36·95	3·07	0·80264	60·04	7·34	52·70	36·98	2·98
102		50·23	44·82	4·96	0·82699	50·33	6·15	44·18	44·91	4·77
103		36·96	55·08	7·96	0·85686	36·97	4·52	32·45	55·10	7·93
104	100·000	95·07	4·86	0·07	0·64913	95·07		95·07	4·86	0·07
105		91·10	8·78	0·12	0·66349	91·07		91·07	8·78	0·15
106		84·76	14·90	0·34	0·68553	84·75		84·75	14·90	0·35
107		80·20	19·20	0·60	0·70085	80·20		80·20	19·20	0·60
108		75·40	23·69	0·91	0·71652	75·35		75·35	23·68	0·97
109		68·91	29·41	1·68	0·73701	68·90		68·90	29·40	1·70
110		52·41	43·26	4·33	0·78733	52·43		52·43	43·28	4·29
111		36·95	55·43	7·63	0·83363	36·92		36·92	55·39	7·70
112		26·47	62·49	11·04	0·86422	26·45		26·45	62·45	11·10
113		16·36	66·86	16·78	0·89272	16·39		16·39	67·01	16·60
114		11·73	67·17	21·10	0·90612	11·73		11·73	67·17	21·10
115		5·20	61·78	33·03	0·92777	5·21		5·21	61·87	32·93
116		2·59	53·65	43·76	0·93944	2·65		2·65	53·62	43·73
117		1·17	44·51	54·32	0·95006	1·39		1·39	44·40	54·21
118		0·58	29·85	69·57	0·96498	0·58		0·58	29·85	69·57
119		0·33	14·97	84·71	0·98263	0·30		0·30	14·97	84·74

of less than 0·1%, a few are higher and lie largely in one region, near the plait points.

Ternary and Quaternary Tie Lines

Tables 2 and 3 show the data, obtained by the methods described above, for six tie lines in the benzene – acetic acid – water ternary system, nine lines in the carbon tetrachloride – acetic acid – water ternary, and 23 lines in the quaternary system. Acetic acid concentrations are shown in some cases; they were obtained by titration, generally in duplicate, of samples with standardized N/5 barium hydroxide, using bromothymol blue as indicator [4].

The tie lines were located with the aid of two charts. The non-aqueous phase specific volume data were plotted on a triangular composition chart, vertices benzene, carbon tetrachloride, and acetic acid + water, 100 cm sides, as lines of constant specific volume at 0·005 ml/g spacing over regions of interest. Specific volumes in the benzene – carbon tetrachloride – water ternary were calculated from the data of SCATCHARD *et al.* [19] on the densities of benzene – carbon tetrachloride mixtures, solubilities in the system being estimated by interpolation between the binary solubilities. For the aqueous phase specific volume (1 cm to 0·002 ml/g) was plotted against weight per cent water (1 cm to 2%).

The phase compositions were determined as follows :

(a) For all ternary tie lines the non-aqueous phase compositions were determined from the specific volume and isotherm data, and for quaternary tie lines numbers 18, 19, 26, 27, 35 and 36 from the specific volume, acetic acid concentration, and isotherm data. Knowing the composition of the initial mixture and that of the non-aqueous phase, the aqueous phase composition was obtained by trial-and-error mass balances.

Table 2. Experimental tie line data for the ternary systems. Benzene (B) – Acetic Acid (A) – Water (W) and Carbon Tetrachloride (C) – Acetic Acid (A) – Water (W)

Benzene – Acetic Acid – Water

Tie line No.	*Initial mixture*			*Wt. aqueous phase / Wt. both phases*	*Non-aqueous phase*		*Aqueous phase*	
	B Wt. %	*A* Wt. %	*W* Wt. %		*Specific Volume at 25°C*	*A* Wt. %	*Specific Volume at 25°C*	*A* Wt. %
1	45·14	15·00	39·86	0·5378	1·14083	2·64 2·68	0·97108	25·64 25·67
2	35·39	17·36	47·25	0·6400	1·14141	—	0·97102	—
3	34·76	25·14	40·10	0·6393	1·13810	—	0·96110	—
4	34·72	26·56	38·72	0·6381	1·13723	—	0·95975	—
5	31·67	51·53	16·80	0·6652	1·10571	—	0·96354	—
6	32·13	52·21	15·67	0·6601	1·10155	26·02 25·98	0·96611	67·91 66·95

Carbon Tetrachloride – Acetic Acid – Water

Tie line No.	*Initial mixture*			*Wt. aqueous phase / Wt. both phases*	*Non-aqueous phase*		*Aqueous phase*	
	C Wt. %	*A* Wt. %	*W* Wt. %		*Specific Volume at 25°C*	*A* Wt. %	*Specific Volume at 25°C*	*A* Wt. %
7	56·42	6·78	36·79	0·4199	0·63253	—	0·98226	—
8	53·73	12·92	33·35	0·4595	0·63479	—	0·96814	—
9	49·59	21·44	28·97	0·4990	0·63895	—	—	—
10	46·47	26·87	26·66	0·5291	0·64229	—	0·94576	—
11	49·31	30·37	20·32	0·4992	0·64792	—	—	—
12	39·53	40·92	19·56	0·6051	0·65617	—	0·92591	—
13	46·75	40·22	13·02	0·5378	0·66767	—	0·91243	—
14	49·21	40·48	10·31	0·5098	0·67720	—	0·90250	—
15	51·15	40·88	7·97	0·4883	0·69040	16·44 16·39	0·88854	67·37 68·86

Table 3. Experimental tie line data for the quaternary system. Benzene (B) – Carbon Tetrachloride (C) – Acetic Acid (A) – Water (W)

Tie line No.	Initial mixture				Wt. aqueous phase / Wt. both phases	Non-aqueous phase		Aqueous phase	
	B Wt. %	C Wt. %	A Wt. %	W Wt. %		Specific Volume at 25°C	A Wt. %	Specific Volume at 25°C	A Wt. %
16	27·96	9·32	25·54	37·18	0·6141	1·01497	—	0·95890	—
17	26·82	8·90	50·69	13·59	0·6279	1·00410	—	0·95629	—
18	36·12	11·95	14·51	37·42	0·5094	1·01659	2·41 2·36	0·97031	26·36 26·35
19	35·04	11·61	22·33	31·03	0·5146	1·01585	4·84 4·83	0·95879	39·08 39·10
20	30·56	9·97	45·55	13·92	0·5512	1·00875	21·65 21·44	0·95335	66·53 66·86
21	20·62	20·57	16·00	42·81	0·5831	0·88988	—	0·97007	—
22	20·06	20·04	24·52	35·38	0·5890	0·89138	—	0·95773	—
23	23·15	23·00	32·64	21·21	0·5124	0·89613	—	0·94635	—
24	17·68	17·62	48·73	15·97	0·6476	0·89984	—	0·94122	—
25	17·97	17·97	51·25	12·81	0·6562	0·90359	—	0·93968	—
26	25·65	25·56	13·65	35·14	—	0·89035	1·90	0·96972	26·49 26·32
27	24·82	24·70	21·21	29·26	0·4894	0·89241	3·93 3·95	0·95754	39·37 39·40
28	21·15	20·97	44·35	13·53	0·5516	0·90282	18·21 18·27	0·94147	66·70 67·06
29	20·80	20·62	47·81	10·77	0·5666	0·90761	24·67 24·64	0·94022	66·54 66·59
30	13·40	40·07	14·84	31·69	0·4583	0·76401	—	0·96321	—
31	12·13	36·06	21·60	30·21	0·5082	0·76693	—	0·95613	—
32	12·53	37·44	30·71	19·32	0·4803	0·77467	—	0·94154	—
33	10·11	30·11	45·60	14·18	0·6005	0·78945	—	0·92704	—
34	9·87	29·71	48·94	11·48	0·6282	0·79899	—	0·91826	—
35	13·78	41·11	12·84	32·27	0·4446	0·76347	1·51 1·47	0·96866	27·11 27·10
36	13·21	39·72	19·99	27·08	0·4584	0·76630	3·05 3·05	0·95584	40·19 40·13
37	11·77	35·00	41·63	11·60	0·5123	0·79313	15·85 15·84	0·92589	67·78 68·08
38	11·51	33·91	44·96	9·62	0·5366	0·80417	20·91 20·96	0·91786	68·98 67·60

(b) For all other quaternary tie lines, the phase compositions were found from the non-aqueous specific volume, the composition of the initial mixture, and the observed phase weight ratio, by trial-and-error calculations.

The bi-nodial compositions obtained are shown in Tables 4 and 5.

Comparison with Published Data

Benzene – acetic acid – water

Hand [9] has published careful and extensive data on this system. His saturation results show somewhat lower solubilities, but the difference is small, and of the same order as his random error. Hand's tie line correlation line is shown in Fig. 5,

Table 4. Equilibrium tie line compositions for the ternary systems. Benzene (B) – Acetic Acid (A) – Water (W) and Carbon Tetrachloride (C) – Acetic Acid (A) – Water (W)

Benzene – Acetic Acid – Water

	Non-aqueous phase			*Aqueous phase*		
Tie Line No.	*B* Wt. %	*A* Wt. %	*W* Wt. %	*B* Wt. %	*A* Wt. %	*W* Wt. %
1	97·22	2·66	0·12	0·37	25·56	73·87
2	97·20	2·68	0·12	0·37	25·62	73·81
3	94·84	4·99	0·17	0·93	36·49	62·58
4	94·20	5·61	0·19	1·04	38·31	60·65
5	74·77	24·05	1·18	10·00	65·35	24·65
6	72·67	25·95	1·38	11·24	65·73	23·03

Carbon Tetrachloride – Acetic Acid – Water

	Non-aqueous phase			*Aqueous phase*		
Tie Line No.	*C* Wt. %	*A* Wt. %	*W* Wt. %	*C* Wt. %	*A* Wt. %	*W* Wt. %
7	99·62	0·36	0·02	0·30	15·12	84·58
8	99·02	0·96	0·02	0·51	26·97	72·52
9	97·93	2·04	0·03	1·07	40·91	58·02
10	97·02	2·94	0·04	1·80	48·02	50·18
11	95·44	4·49	0·07	3·24	56·22	40·54
12	93·14	6·76	0·10	5·60	62·53	31·87
13	89·90	9·92	0·18	9·50	66·39	24·11
14	87·21	12·54	0·25	12·77	67·27	19·96
15	83·32	16·26	0·42	17·41	66·70	15·89

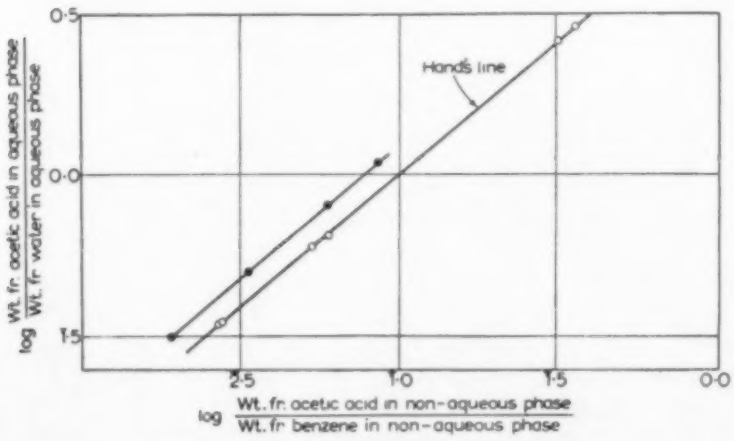

Fig. 5. ○ This work ● Bektourov

Table 5. Equilibrium tie line compositions for the quaternary system. Benzene (B) – Carbon Tetrachloride (C) – Acetic Acid (A) – Water (W).

	Non-aqueous phase				*Aqueous phase*			
Tie Line No.	*B* Wt. %	*C* Wt. %	*A* Wt. %	*W* Wt. %	*B* Wt. %	*C* Wt. %	*A* Wt. %	*W* Wt. %
16	71·11	23·87	4·87	0·15	0·84	0·18	38·53	60·45
17	54·79	19·21	24·77	1·23	10·25	2·79	66·05	20·91
18	73·25	24·26	2·39	0·10	0·44	0·12	26·15	73·29
19	71·31	23·71	4·83	0·15	0·84	0·20	38·84	60·12
20	58·24	19·78	21·08	0·90	8·03	1·99	65·47	24·51
21	49·00	49·05	1·89	0·07	0·33	0·21	26·09	73·37
22	47·90	48·20	3·79	0·11	0·63	0·39	38·98	60·00
23	45·25	45·95	8·57	0·23	2·12	1·16	55·54	41·18
24	39·44	42·23	17·71	0·62	5·84	4·23	65·61	24·32
25	36·45	39·52	23·00	1·03	8·29	6·68	66·05	18·98
26	49·08	48·95	1·90	0·07	0·30	0·25	26·37	73·08
27	47·96	47·99	3·94	0·11	0·66	0·39	39·24	59·71
28	39·74	41·47	18·14	0·65	6·03	4·30	65·67	24·00
29	36·35	38·27	24·23	1·15	8·91	7·12	65·85	18·12
30	24·57	73·61	1·78	0·05	0·20	0·43	30·28	69·09
31	24·22	72·70	3·01	0·07	0·43	0·60	39·59	59·38
32	22·92	70·02	6·92	0·14	1·29	2·17	56·46	40·08
33	20·10	64·64	14·85	0·41	3·46	7·14	66·06	23·34
34	18·58	61·01	19·71	0·70	4·72	11·18	66·24	17·86
35	24·67	73·79	1·49	0·05	0·19	0·35	27·00	72·46
36	24·08	72·80	3·05	0·07	0·38	0·69	39·98	58·95
37	20·19	63·63	15·73	0·45	3·75	7·75	66·29	22·21
38	19·00	59·63	20·60	0·77	5·44	11·29	66·01	17·26

together with the points representing the present work. The agreement shown is possible, despite the difference in isotherms, as the HAND correlation only involves the concentrations of the major components. Data of BEKTOUROV [2] are also shown; his points lie on a line parallel to, but distinct from, the present results, and in view of the coincidence of the latter and of HAND's results, BEKTOUROV's are considered less reliable.

Carbon tetrachloride – acetic acid – water

SMITH and BERMAN [23] determined this isotherm as part of a wider investigation, and their results are consistent with the present, except for the aqueous phase with acetic acid concentrations below 50%, where their results appear subject to rather large experimental error.

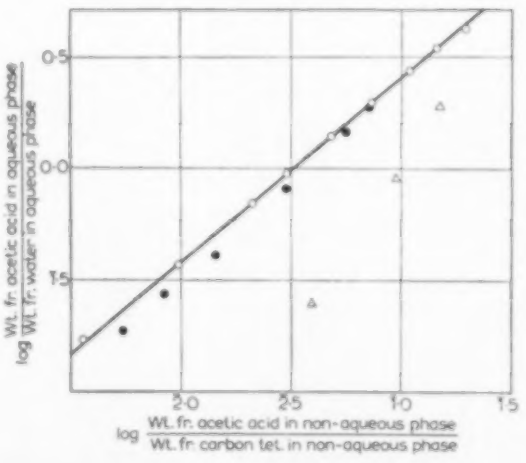
0·5
0·0
1·5
2·0
2·5
1·0
1·5
log Wt. fr. acetic acid in aqueous phase / Wt. fr. water in aqueous phase
log Wt. fr. acetic acid in non-aqueous phase / Wt. fr. carbon tet. in non-aqueous phase

FIG. 6.

○ This work ● BEKTOUROV △ SALETORE *et al.*

Saturation results of SALETORE, MENE and WARHADPANDE [18] at 27°C scatter about the present data. They also reported three tie lines, shown on a HAND plot together with the present results in Fig. 6. These lines were also determined by the synthetic method, and as the composition of one phase only of one tie line fell within their experimental isotherm, they must be subject to considerable error.

BEKTOUROV's data [2] are also shown in Fig. 6, and again diverge from the present results.

SEIDELL and LINKE [21] quote saturation compositions ascribed to SIGGIA and HANNA [22]. These lie well within the homogeneous region as defined by the present results, and reference to the original publication showed that these compositions had no connection with the isotherm, and merely represented certain synthetic mixtures.

VOL. 6 956/57

THE SYSTEM BENZENE – CARBON TETRACHLORIDE – WATER

The quaternary system studied includes three ternary systems with miscibility gaps : benzene – acetic acid – water, carbon tetrachloride – acetic acid – water, and benzene – carbon tetrachloride – water. While experimental results are presented for the first two of these, no attempt was made to obtain any for the last. This is a double non-consolute pair system with very low solubilities (the highest binary solubility being that of benzene in water, 0·18 g per 100 g), so that reliable results would be difficult to obtain, and it was not expected that they would be required in the present study. For many purposes the tie lines in this system may be regarded as passing through the water apex, and for cases in which this concept is inadequate, the distribution to be expected may be derived [17].

DISCUSSION

The results presented for the isotherm of the quaternary system show that the cloud point titrations were generally reproducible to within 0·1% or better, and with the technique described it may be possible to improve the reproducibility even further by more careful work, e.g. repeat titrations. Such extra precautions were not taken in the present work as the nature of the isotherm made correction of titration results possible by the methods described.

Such precision is not, however, attainable over all the surface. Table 1 shows that for certain points larger corrections had to be made. These points lie in the region of the plait points, and during titration here unexpected phenomena were observed, which will be described briefly, as they may lead to confusing results. As the titration proceeded a blue haze developed in the solution, which became marked, and rendered the solution almost opaque ; this was followed by the sudden appearance of a very heavy white cloud. As the development of the blue colour was very gradual, while the advent of the white cloud was most marked, and seemed reproducible, the latter event was taken to be the attainment of saturation. When, after weighing and slight heating to clear them, the solutions had been returned to the thermostat, they became definitely cloudy, but gentle twirling of the flask would be sufficient to clear them, suggesting that if the correct end point had been exceeded, it had been exceeded by very little. Plotting the results as above suggested that the over-titration was appreciable, and attempts were made to avoid this, by stopping the titration, and shaking, at frequent intervals after the first appearance of the blue haze, and awaiting the appearance of a definite cloud point. This occurred occasionally, but on the whole this technique was no more successful than the original. As these phenomena were confined to the cloud point region, and as this region was of little interest for the purposes of the present work, no further investigation was made.

Other workers, e.g. HAND [9], have drawn attention to anomalous behaviour in this region, and as he pointed out, this emphasises the assumption implicit in the synthetic method that the cloud point curve is identical with the equilibrium saturation curve. This assumption is unnecessary in the analytical method, but that method can not often be applied, and generally lacks precision. This criticism would seem to be borne out by the present results for the tie lines, where there are comparatively great discrepancies between the acetic acid concentrations, as found by titration, and those calculated. It seems likely

that the titrated, rather than the calculated figures were less accurate, as

(i) The experimentally determined aqueous phase density checks with the calculated compositions;

(ii) At the higher acid concentrations the repeat titrations are inconsistent, and several figures are above the limits of heterogeneity as found by the cloud point titrations;

(iii) A numerical check is available for those lines of group (a) above, for which a neat separation was achieved, and for which the other data required are known to be reliable. For such lines the ratio weight of aqueous phase to weight of both phases was calculated from the phase compositions and the composition of the initial mixture. These figures, together with those obtained experimentally, are shown in Table 6. The difference between the two sets is small, and of the order to be expected from the methods employed. For eight of the eleven tie lines the calculated ratios are greater than the experimental values, but a statistical test [8] showed that there was no consistent difference, and the two methods of calculation should lead to consistent results.

Extensive experiments were carried out to trace the source of the discrepancies in the acid concentrations. These showed that titration gave the correct amount of acid in the samples submitted, and that the overall composition of the equilibrium mixture remained constant during a run, so that the rise in acid concentration took place during sampling, by evaporation of the more volatile components, as the phase was sampled directly into a large vessel suitable for the titration. Avoidance of such an error would be difficult, and this would tend to restrict the precision of an analytical method. Although the acid titration errors were large compared to those of the methods adopted, they represent at most 3% errors in the acid mass balances, and hence would have been considered acceptable in most liquid – liquid equilibrium work.

In the method of tie line determination adopted, a sample was only required for the density measurements, and as this was pushed directly into a pycnometer, there was no similar opportunity for evaporation and consequent error. For the purposes of Table 6, acid titration results were accepted for acid concentrations below 5%, as here comparatively large samples were taken, and the errors involved were of the same order as those of the other measurements. Some estimate of the precision of this method of tie line determination may be obtained from Table 6. The average difference in the two sets of weight ratios is 0·00015, which corresponds to an error of 0·03% in the mass balance of a component in terms of the total weight. While this is certainly an underestimate of the average error

Table 6. Comparison of calculated and observed values of ratio $\frac{\textit{Wt. aqueous phase}}{\textit{Wt. both phases}}$

Line	$\frac{\textit{Wt. aqueous phase}}{\textit{Wt. both phases}}$ (calculated)	$\frac{\textit{Wt. aqueous phase}}{\textit{Wt. both phases}}$ (observed)
2	0·6397	0·6400
4	0·6385	0·6381
5	0·6654	0·6652
8	0·4597	0·4595
9	0·4991	0·4990
15	0·4881	0·4883
18	0·5100	0·5094
19	0·5147	0·5146
27	0·4892	0·4894
35	0·4450	0·4446
36	0·4587	0·4584

VOL. 6 1956/57

for all the tie lines (as those included in the table were necessarily not a representative sample) the average error should be of the order of 0·1%, the figure originally aimed at.

At the same time, the practical convenience of the technique described should be stressed, particularly for ternary systems, where, if the phase weight ratios are accepted as reliable, no samples are needed, and the only measurements required are the weights of the components added and of one phase. It is therefore suggested that this method represents advances over the conventional methods, both in convenience and in accuracy.

Relationship between the Ternary and Quaternary Systems

Brancker, Hunter and Nash [4] have studied the quaternary system acetic acid – chloroform – acetone – water at 25°C, which is of the type illustrated in Fig. 1 (a). The quaternary tie lines were found to lie on the intersection of a plane passing through a tie line in a ternary system containing the pair of non-consolute components and the opposite apex of the tetrahedron with a similar tie line plane based on the other ternary system containing the pair of non-consolute components.

Pratt and Glover [16] determined tie lines in a similar system, actone – acetaldehyde – vinyl acetate – water at 20°C, which seem to be in fair agreement with those expected from the Brancker, Hunter and Nash relationship. Brancker [5] claimed to obtain better agreement by a different method of calculation, but this does not appear to be valid.

No other quaternary systems of this type have as yet been investigated in sufficient detail. The application of the Brancker, Hunter, and Nash correlation to the present system gave systematic deviations between actual and calculated results outside the expected limits of experimental error and it would appear that these tie line relationships do not apply to this system [17].

Chang and Moulton studied four quaternary systems of the type illustrated in Fig. 1 (b). Of these the system water – ethyl *iso*valerate – ethyl alcohol – benzene was studied in some detail and its quaternary tie lines were found to lie in planes passing through tie lines in the ternary system containing the two non-consolute pairs. In Fig. 7 the line *FG* is a tie line in the two non-consolute pair ternary *BCD*, and the line *EC* is this line extended. The plane through *EFGC* and the opposite apex *A*, namely plane *ECA*, is then a quaternary tie line plane, i.e. a quaternary tie line through any point in the plane lines within that plane. Chang and Moulton also obtained distribution data for three similar systems, which supported the existence of such quaternary tie line planes, within experimental error.

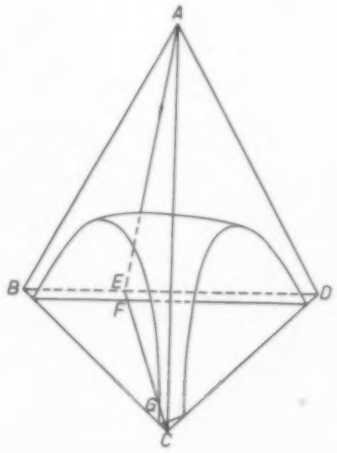

Fig. 7.

Prince [17] recalculated Brown's [6] quaternary tie line data for the system aniline – benzene – cetane – *cyclo*hexane at 25°C and concluded that the tie line relationship suggested by Chang and Moulton might apply to this system. Moreno and Gonzales [12] investigated the system methanol – carbon disulphide – oleic acid – olive oil at 25°C and treated this as if it were a quaternary system of type (b). They claimed that the Chang and Moulton relationship applied to this case.

If the Chang and Moulton relationship applies to the present system then the quaternary tie lines must be in planes through the water and acetic acid apices, namely planes of constant

Table 7. Ratio carbon tetrachloride to benzene for quaternary tie lines

Tie Line	*Overall Mixture*	*Non-aqueous Phase*	*Aqueous phase*
18	0·3308	0·3312	0·273
19	0·3313	0·3325	0·238
16	0·3333	0·3357	0·214
20	0·3262	0·3396	0·248
17	0·3318	0·3506	0·272
21	0·9976	1·0010	0·636
26	0·9965	0·9973	0·833
22	0·9990	1·0063	0·619
27	0·9952	1·0006	0·591
23	0·9935	1·0155	0·547
24	0·9966	1·0707	0·724
28	0·9915	1·0435	0·713
25	1·0000	1·0842	0·806
29	0·9913	1·0528	0·799
35	2·983	2·991	1·84
30	2·990	2·996	2·15
31	2·973	3·002	1·39
36	3·007	3·023	1·82
32	2·988	3·055	1·68
33	2·978	3·216	2·06
37	2·974	3·152	2·07
34	3·010	3·284	2·37
38	2·946	3·138	2·07

carbon tetrachloride/benzene ratio and this ratio must be the same for both conjugate phases and for the overall mixture from which the conjugate phases were derived. If in Fig. 7 the apices *A*, *B*, *C* and *D* represent acetic acid, benzene, water, and carbon tetrachloride, respectively, then the Chang and Moulton quaternary tie line plane will be the plane *ACGFE*, and in this plane the ratio of *B* to *D*, namely benzene to carbon tetrachloride, will remain constant.

In Table 7 this ratio, as carbon tetrachloride to benzene, is given for the overall mixture and for the conjugate phases of the quaternary tie lines, arranged in order of increasing acetic acid content. This ratio deviates in both phases in a systematic manner from the overall ratio, while there is no such deviation in the results of Chang and Moulton. As benzene and carbon tetrachloride have very different densities (0·87 and 1·59 respectively) and as density was employed to determine the ratio of these components in the non-aqueous phase, the determined ratio data for this phase are believed accurate. In the aqueous phase, however, the concentrations of both these components are low, and the ratio of these in this phase will be subject to fairly large errors.

As far as the present system is concerned it would appear that the Chang and Moulton tie line correlation is only an approximation. Even if this, or a similar correlation were valid generally for quaternary systems of type 1 (b), it would not be sufficient to predict quaternary equilibria from data for the ternary systems only (as is possible with the Brancker, Hunter, and Nash correlation for type 1 (a) systems). Correlations which enable such predictions to be made have been discussed in more detail by Prince [17].

VOL 6 1956

References

[1] Bancroft W. D. *Phys. Rev.* 1895 **3** 21, 115, 193.

[2] Bektourov S. A. *Zh. Obs. Khimit* 1939 **9** 419 ; as quoted by Seidell [20].

[3] Bonner W. D. *J. Phys. Chem.* 1910 **14** 738.

[4] Brancker A. V., Hunter T. G., and Nash A. W. *J. Phys. Chem.* 1940 **44** 683.

[5] Brancker A. V. *Ind. Chem. Mfr.* 1951 **27** 243.

[6] Brown T. F. *Industr. Engng. Chem.* 1948 **40** 103.

[7] Chang Y. C. and Moulton R. W. *Industr. Engng. Chem.* 1953 **45** 2350.

[8] Fisher R. A. *Statistical Methods for Research Workers* (11th ed.) p. 174. Edinburgh, Oliver and Boyd, 1950.

[9] Hand D. B. *J. Phys. Chem.* 1930 **34** 1961.

[10] Kirk P. L. *Quantitative Ultramicroanalysis* London, Chapman and Hall, 1950.

[11] Miller W. L. and McPherson R. H. *J. Phys. Chem.* 1908 **12** 706.

[12] Moreno J. M. M. and Crespi Gonzales M. A. *An. Real Soc. Espăn. Fis. Quim.* (Madrid) 1948 **4B** 391.

[13] Othmer D. F. and Tobias P. E. *Industr. Engng. Chem.* 1942 **34** 690.

[14] Othmer D. F., White R. E., and Trueger E. *Industr. Engng. Chem.* 1941 **33** 1240.

[15] Palmer W. G. *Experimental Physical Chemistry* p. 185. Cambridge University Press, 1941.

[16] Pratt H. R. C. and Glover S. T. *Trans. Ind. Inst. Chem. Engrs.* (London) 1946 **24** 54.

[17] Prince R. G. H. *Chem. Eng. Sci.* 1954 **3** 175.

[18] Saletore S. A., Mene P. S., and Warhadpande U. R. *Trans. Ind. Inst. Chem. Engrs.* 1948 **2** 16.

[19] Scatchard G., Wood S. E., and Mochel J. M. *J. Amer. Chem. Soc.* 1940 **62** 712.

[20] Seidell A. *Solubilities of Organic Compounds* (3rd ed.) New York, Van Nostrand, 1941.

[21] Seidell A. and Linke W. F. *Solubilities of Inorganic and Organic Compounds* (Suppl. to 3rd ed.) New York, Van Nostrand, 1952.

[22] Siggia S. and Hanna J. C. *Analyt. Chem.* 1949 **21** 1086.

[23] Smith H. A. and Berman M. *J. Amer. Chem. Soc.* 1937 **59** 2390.

VOL.
6
956/57

Chemical Engineering Science, 1957, Vol. 6, pp. 262 to 268. Pergamon Press Ltd.

On shape factors for irregular particles—I

The steady state problem. Diffusion and reaction

R. Aris

The Mathematical Institute, 16 Chambers Street, Edinburgh 1

(*Received* 20 *January* 1957)

Abstract—The problem of heat or matter transfer for a bed of spherical particles has been fully solved by Amundson. In this paper we consider the modifications which must be made in steady state solution when the bed may consist of irregularly shaped particles. Considering the case of diffusion limitation of a first order reaction it is shown that the results for all shapes will lie close together if the characteristic dimension of the particle is taken to be v_p/s_x, the ratio of its volume to its external surface area.

Résumé—Le problème de transfert de chaleur ou de matière pour un lit de particules sphériques a été résolu par Amundson. Dans cet article, l'auteur considère les modifications susceptibles d'être apportées à la détermination de l'état de régime quand le lit est constitué par des particules de formes irrégulières. En considérant le cas de limitation par diffusion d'une réaction du 1° ordre l'auteur montre que les résultats sont voisins, si la dimension caractéristique de la particule est égale à V_p/S_x (rapport de son volume à sa surface externe).

VOL 6 1956

1. Introduction

The notion of a shape factor for particles of irregular shape has been introduced empirically in several contexts interesting to the chemical engineer. Leva [6], for example, in studying pressure drop in packed beds introduces the shape factor $\phi = (36\,\pi)^{\frac{1}{3}}\, v_p^{\frac{2}{3}}/s_x$ where v_p is the volume of the particle and s_x its surface area. This factor is unity for the sphere and between 0 and 1 for all other shapes, and using it he is able to improve the correlation of pressure drop versus Reynold's number. The introduction of such a factor should be somewhat tentative for mathematical considerations give no hope of a single parameter completely reconciling the solutions of a particular problem for two distinct shapes of particle. However the practical value of so simple an adjustment of results is very great even though a small margin of error is introduced. It is our purpose here to examine two problems in packed beds and show the extent to which such a practice can be justified.

The first problem concerns the diffusion limitation of a first order reaction taking place on the surface of a porous catalyst. This problem was first solved by Thiele [8] who gave two curves one for flat plates and another for spherical particles. His solution and the physical background has received an extended treatment by Wheeler [9] and is described and used in Hougen and Watson's well-known treatise [4]. In sections 2, 3 some justification is given for using as the characteristic linear dimension of an arbitrary shaped particle the ratio v_p/s_x, when a single curve for the effectiveness factor may be used with good accuracy. In section 4 the equivalent particle diameter for a mixture of particles is discussed.

The second problem, to be considered in Part II, is that of the fixed bed heat exchanger or ion exchange column. It shows well the pitfalls of endeavouring to use a single shape factor, for though at first sight the same specification of characteristic length appears to give a measure of agreement between various shapes, this agreement is shown to be spurious. However a shape factor can be found in this case which compares the " softening " of a sharp temperature or concentration wave passing through the bed for various shapes of particle. Since a very

general problem has been investigated by AMUNDSON [1] for spheres we follow his notation and methods some distance in section 6. Section 7 gives a method of calculating the shape factor for this problem and the final paragraph discusses the relation between the two problems treated here and that solved completely by AMUNDSON for spherical particles.

2. SIMULTANEOUS DIFFUSION AND REACTION IN CATALYST PLATES

To introduce this problem we will first give THIELE's solution for the flat plate in terms of the notation to be used here. Consider a porous catalyst particle in the form of a thin flat plate with sealed edges so that the flow of reactants is always perpendicular to the faces. Take a co-ordinate x in this direction of flow and let $x = 0$ denote the centre plane of the plate and $x = \pm a$ the faces. We consider for simplicity a first order reaction with no volume change whose rate is proportional to the concentration c of one of the reactants. Let

$c = c(x)$ = concentration of the reactant in the plane

$c_s = c(a)$ = its concentration at the surface

D = diffusion coefficient of the reactant within the particle

σ = active catalyst surface/unit catalyst volume

k = reaction rate constant/unit active catalyst area.

Taking a matter balance over an element between the planes $x \pm \frac{1}{2} dx$ we derive in the usual way

$$D \frac{d^2c}{dx^2} = k \sigma c \tag{1}$$

By symmetry there is no flow of reactant across the centre plane

i.e. $$\frac{dc}{dx} = 0, \; x = 0 \tag{2}$$

and at the surface

$$c = c_s, \; x = a. \tag{3}$$

These equations determine the distribution of concentration within the particle and we have

$$c = c_s \frac{\cosh \lambda x}{\cosh \lambda a} \text{ where } \lambda = k\sigma/D \tag{4}$$

and the flow into the particle per unit area is

$$\left[D \frac{dc}{dx} \right]_{x=a} = D c_s \lambda \tanh \lambda a. \tag{5}$$

Consider now a bed of such particles through which the reactants are flowing, the particles being sufficiently small for the concentration c_s to be constant around any single particle.

Let z = co ordinate of bed depth

A = area of bed

α' = voidage of bed

v_f = volume rate of flow of reactants.

Then a matter balance over an elementary section of the bed between the plane $z \pm \frac{1}{2} dz$, gives

$$[v_f c_s]_{z - \frac{1}{2} dz} - [v_f c_s]_{z + \frac{1}{2} dz} = (1 - \alpha') A \, dz \frac{1}{a} \left[D \frac{dc}{da} \right]_{x=a}$$

In deriving this we have made use of the facts :

$(1 - \alpha') A \, dz$ = volume occupied by catalyst particles

a^{-1} = area through which reactant flows in/volume of catalyst.

Using equation (5) and taking the limit $dz \to 0$ we have for c_s the equation

$$- \frac{v_f}{A(1 - \alpha')} \frac{dc_s}{dz} = \frac{1}{a} (D \lambda \tanh \lambda a) c_s. \tag{6}$$

If there were no diffusion limitation and all the catalyst surface area were available to the reactant a similar matter balance would give

$$- \frac{v_f}{A(1 - \alpha')} \frac{dc_s}{dz} = k \sigma c_s \tag{7}$$

Comparing equations (6) and (7) we see that full allowance can be made for the diminished rate of reaction if in (7) k is replaced by ηk, where

$$\eta = \frac{\tanh \lambda a}{\lambda a} ; \tag{8}$$

η is called the effectiveness factor.

Cast in this form the problem is immediately amenable to generalisation. We may set up the equations for a particle of arbitrary shape, to replace equations (1), (2) and (3) for the flat plate and then calculate the average rate of flow across the particle surface to replace equation (5).

3. Diffusion and Reaction in Catalyst Particles of Arbitrary Shape

Consider a catalyst particle of arbitrary shape, but as before sufficiently small for the concentration of the reactant, c_s, to be sensibly constant over its surface. Let ξ, η, ζ be Cartesian coordinates in the space of the particle which we take to occupy a region R and be bounded by a surface S. These space variables correspond to the variable x above.

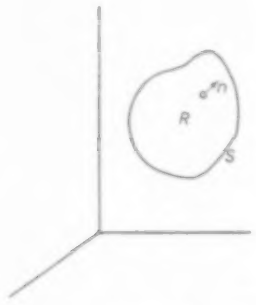

Fig. 1. The general particle.

Let v_p = volume of particle,
dv = element of volume,
s_x = external surface area of particle,
ds = element of surface area,
$\partial/\partial n$ = differentiation along the outward normal n_s to S.
∇^2 = the Laplacian operator,

A matter balance within the volume of the particle now gives for the concentration $c = c(\xi, \eta, \zeta)$ the equation

$$\nabla^2 c = \lambda^2 c \text{ in } R, \tag{9}$$

where again $\lambda^2 = k\sigma/D$, and on the surface

$$c = c_s \text{ on } S. \tag{10}$$

Equations (9) and (10) replace (1)-(3) and their solution gives the concentration distribution within the particle. The total flow into the particle over the surface is

$$D\iint_S \frac{\partial c}{\partial n}\, ds = D\iiint_R \nabla^2 c\, dv = k\sigma \iiint_R c\, dv \tag{11}$$

by Green's formula and the equation (9).

Let $\chi(\xi, \eta, \zeta)$ denote the solution of (9) which has boundary values $\chi = 1$ on S. Then $c(\xi, \eta, \zeta) = c_s \chi(\xi, \eta, \zeta)$ and a matter balance similar to equation (6) gives

$$-\frac{v_f}{A(1-\alpha')}\frac{dc_s}{dz} = \left[\frac{1}{v_p}\iiint_R \chi\, dv\right] k\sigma c_s \tag{12}$$

from which it is evident that

$$\eta = \frac{1}{v_p}\iiint_R \chi\, dv \tag{13}$$

where $$\nabla^2 \chi = \lambda^2 \chi \text{ in } R$$

and $$\chi = 1 \text{ on } S. \tag{14}$$

The effectiveness factor η depends on the shape of the region R and on the parameter λa, where a is some characteristic dimension of the particle. The problem of a shape factor is the problem of choosing the value of a appropriate to the given shape of the particle so that the functions $\eta(\lambda a)$ shall be as close together as possible for all shapes.

For certain common shapes equations (13) and (14) can be readily solved, taking for a an obvious dimension. For example

(i) Flat plates : a = half thickness :
$\eta = \tanh \lambda a / \lambda a$

(ii) Cylinder with ends sealed : a = radius :
$\eta = 2 I_1(\lambda a)/\lambda a\, I_0(\lambda a)$

(iii) Sphere : a = radius :
$\eta = 3(\lambda a \coth \lambda a - 1)\lambda^2 a^2$

(iv) Cylinder with porous ends : a = radius, length = $2a/p$:

$$\eta = 1 - \frac{32}{\pi^2}\sum_{m=1}^{\infty}\sum_{n=0}^{\infty}\frac{1}{(2n+1)^2 j_m^2}\,\frac{\lambda^2 a^2}{\lambda^2 a^2 + j_m^2 + (2n+1)^2 p^2 \pi^2}$$

In the above $I_n(x)$ is the modified Bessel function

VOL 6 1956

of order n, and j_m is the mth zero of the Bessel function $J_0(x)$.

When $\lambda a \to 0$, $\eta \to 1$ as it should, for $\lambda a = 0$ implies no limitation by diffusion. When $\lambda a \to \infty$, $\eta \to m/\lambda a$ where in the first three cases we have $m = 1, 2, 3$, respectively. Now in all three cases a/m is the ratio v_p/s_x so that for large λa, $\eta \sim (\lambda v_p/s_x)^{-1}$. Thus in three important cases we see that by setting $a = v_p/s_x$ the functions η become identical for large and small λa. Before suggesting that it is satisfactory always to set $a = v_p/s_x$ we should do two things. Firstly estimate the error likely to be introduced for intermediate values of λa and secondly show that for an arbitrary shape we always have $\eta \sim (\lambda v_p/s_x)^{-1}$.

For the first let us set

$$\Lambda = \lambda v_p/s_x = (v_p^2 k\sigma/s_x^2 D)^{\frac{1}{2}}$$

then for

(i) flat plate : $\eta = \tanh \Lambda/\Lambda$ (15)

(ii) cylinder : $\eta = I_1(2\Lambda)/\Lambda I_0(2\Lambda)$ (16)

(iii) sphere : $\eta = (3\Lambda \coth 3\Lambda - 1)/3\Lambda^2$ (17)

Table 1. *Effectiveness factor η for various shapes*

Λ	η		
	Flat plate	*Cylinder*	*Sphere*
0·1	·997	·995	·994
0·2	·987	·981	·977
0·5	·924	·892	·876
1	·762	·698	·672
2	·482	·432	·416
5	·200	·197	·187
10	·100	·100	·097

From this table of values it is clear that the functions $\eta(\Lambda)$ follow one another quite closely, the greatest difference between spheres and flat plates being approximately 0·09. To obtain estimates of the divergence in the general case would be an excessively difficult task, equivalent to solving the problem completely, but this table gives us some confidence in the use of the parameter Λ.

As an illustration of the variation of η with shape at constant Λ we may mention the spherical

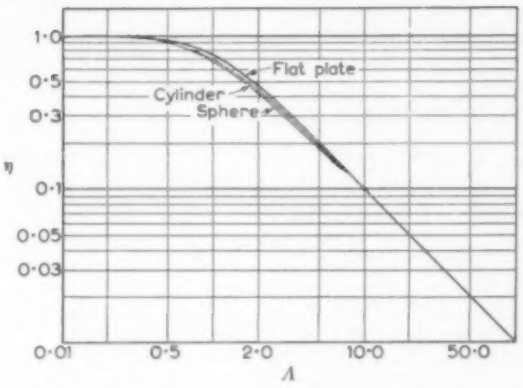

Fig. 2. Effectiveness factor for various shapes

shell. In this case we assume that the active catalyst is a spherical shell between the radii a and ρa. Then $s_x = 4\pi a^2$ and $v_p = 4\pi a^3(1-\rho^3)/3$ so that $\Lambda = \lambda a(1-\rho^3)/3$. Setting $(1-\rho^3)\Lambda' = 3(1-\rho)\Lambda$ we have

$$\eta = \frac{3(1-\rho)}{(1-\rho^3)} \frac{1}{\Lambda'^2} \frac{(1-\rho)^2(\Lambda' - \tanh\Lambda') + \rho\Lambda'^2 \tanh\Lambda'}{(1-\rho)\tanh\Lambda' + \rho\Lambda'}.$$

When $\rho = 0$, $\Lambda' = 3\Lambda$ and η reduces to the expression for a sphere, (17), whilst when $\rho = 1$ we have $\Lambda' = \Lambda$ and the expression for a flat plate, (15). Taking $\Lambda = 1$ at which point we have noticed the greatest difference, we get the following values :

ρ	0	·25	·5	·75	1·0
η	·672	·675	·691	·723	·762

As regards the asymptotic behaviour of η it is at once evident that $\Lambda = \lambda v_p/s_x$ is likely to be a uniformising parameter. For large values of Λ imply a strong diffusion limitation, i.e. the reaction rate is so much faster than the diffusion rate that the concentration falls off extremely rapidly. In these circumstances when only a thin surface layer is really operative it is effectively a flat plate, and $\eta = \frac{1}{v_p}\int\int\int_R \chi\, dv$, receiving its main contribution from the immediate neighbourhood of the surface, becomes proportional to s_x/v_p.

More rigorously, we consider S to be composed of a finite number of smooth surfaces as, for example, is the finite cylinder with its curved surface and flat ends. In the neighbourhood of any smooth part of S we may introduce coordinates such that S is the surface of constant ξ (say $\xi = a$) then $\partial/\partial n = \partial/\partial\xi$ and a solution valid in the immediate neighbourhood of S for large λ is

$$\chi = e^{-\lambda(a-\xi)} + \psi(\xi, \eta, \zeta),$$

where ψ and ψ_ξ are negligibly small on S. Since drops to zero very rapidly it is sufficient to have a solution valid in the immediate neighbourhood of S and

$$\left.\begin{aligned}\eta &= \frac{1}{v_p}\iiint_R \chi \, dv = \frac{1}{\lambda^2 v_p}\iiint_R \nabla^2 \chi \, dv \\ &= \frac{1}{\lambda^2 v_p}\iint_S \frac{\partial \chi}{\partial \xi}\, ds = \frac{1}{\lambda v_p}\iint_S ds = \frac{s_x}{\lambda v_p}\end{aligned}\right\} \quad (18)$$

These considerations give a fair measure of confidence in using the mean curve of figure 2 for all shapes. In this figure the curves of table 1 are given to give some measure of the possible error.

A remark may be made as to the use of the shape factor $\phi = (36\pi v_p^2)^{\frac{1}{3}}/s_x$ introduced by Leva. If the general particle of volume v_p is replaced by a sphere of radius a of the same volume, i.e. $a = (3v_p/4\pi)^{\frac{1}{3}}$ and the parameter $\Lambda^* = \lambda a/3$ for the sphere is used, no allowance has been made for the difference in shape between the particle and the sphere. If however we take $\Lambda = \phi\Lambda^* = \frac{1}{3}\lambda(3v_p/4\pi)^{\frac{1}{3}}(36\pi v_p^2)^{\frac{1}{3}}/s_x = \lambda v_p/s_x$ we arrive at our parameter. On a log-log plot of η versus Λ such as in Fig. 2 the points corresponding to Λ for the particle and Λ^*, the value of Λ for the sphere of equal volume, are separated by a constant difference $\log\phi$. It is clear from this that of all catalyst particles of given volume diffusion limitation is most severe in a spherical one.

4. Mixtures of Particle Size

If the bed is composed of a mixture of particles of various sizes we may enquire whether it is possible to use a mean particle size to describe the overall performance of the bed. Leva in his studies of pressure drops [6] suggests a mean radius a, given by $a^{-1} = \Sigma w_i a_i^{-1}$ where w_i is the weight fraction of the i^{th} size and a_i the radius of the sphere of equal volume. We shall see that this is satisfactory in so far as any mean can be satisfactory. The bed is assumed to be homogeneous in the sense that a sample from any part of it would show approximately the same proportion f_i of the packed volume to be occupied by particles of the i^{th} size. We have $\Sigma f_i = 1$ and if the density of all particles is the same $w_i = f_i$.

To account correctly for the mixture of sizes we must take each size and calculate the corresponding value of Λ say Λ_i, then

$$\eta = \Sigma f_i \eta(\Lambda_i) \quad (19)$$

If this value of η corresponds to a particular value of Λ, say $\bar{\Lambda}$, we have from the relation $v_p/s_x = \bar{\Lambda}/\lambda$ a value for the equivalent mean size of the particles. Equation (19) is however quite general and can be used for a mixture both of shapes and sizes, nor should it be excessively difficult to use in practice.

There are however two cases in which a mean size can be calculated before finding the effectiveness. The first is the trivial case when diffusion is not limiting for any size of particle, $\Lambda < 0{\cdot}1$ for even the largest particle. In this case any mean size will serve for η will be 1 in all cases. The second case is when diffusion is limiting even in the smallest particles, i.e. $\Lambda > 5$ for all sizes. In this case $\eta(\Lambda_i) \doteqdot \Lambda_i^{-1}$ and as we have seen $\Lambda = \phi\Lambda^* = \phi\lambda a/3$ where a is the radius of the sphere of equal volume. From (19)

$$\eta = \Sigma f_i \Lambda_i^{-1} = (3/\lambda\phi)\,\Sigma f_i a_i^{-1} = 3/\lambda\phi a$$

where a is the correctly defined mean value. Hence

$$a = (\Sigma f_i a_i^{-1})^{-1} \quad (20)$$

is the appropriate mean.

If the range of sizes involves that diffusion is limiting in some particles but not in others then any mean size calculated before the effectiveness

will be inaccurate. For example if the mixture is in equal volume proportions of five sizes, $f_i = 0{\cdot}2$, giving $\Lambda_i = \frac{1}{2}, 1, 2, 5, 10$, the value of Λ calculated from the mean (20) is 1·316. This gives $\eta = 0{\cdot}658$ which is widely different from the value 0·397 calculated from (19).

5. External Diffusion Limitations

A remark may here be added, in view of its connection with the problem which follows, as to the additive effect of a diffusion limitation through the relatively stagnant film surrounding a pellet in the fluid stream. This is often termed a mass transfer limitation and has been considered by Hougen and Watson [4] and others.

We assume that because of the presence of a thin film (of thickness h) of stagnant fluid around the particle the surface concentration c_s is not quite equal to the concentration c_f in the body of the flowing reactant. If h is small we may assume that the flow of reactant is linear and if x is a coordinate through the thickness of the film $D_f \dfrac{d^2c}{dx^2} = 0$, where D_f is the diffusion coefficient in the film. Then $c = c_f$, $x = 0$; $c = c_s$, $x = h$ and $c(x) = (x/h)(c_s - c_f) + c_f$. Thus for the inward flow through the film we have

$$-D_f \frac{dc}{dx} = D_f \frac{c_f - c_s}{h} = \frac{v_p}{s_x} \eta k\sigma c_s$$

Thus $$c_f = c_s \left(1 + \frac{v_p h k\sigma}{s_x D_f} \eta\right) \quad \text{and}$$

$$\eta k \sigma c_s = k \sigma \left(\frac{1}{\eta} + \frac{v_p h k\sigma}{s_x D_f}\right)^{-1} c_f.$$

A matter balance in the bed then gives

$$-\frac{v_f}{A(1-\alpha')} \frac{dc_f}{dz} = E k\sigma c_f$$

where E, the overall effectiveness is given by

$$\frac{1}{E} = \frac{1}{\eta} + \frac{v_p h k \sigma}{s_x D_f} = \frac{1}{\eta} + \frac{1}{\eta_f} \qquad (21)$$

In such a situation as this the reciprocal of the effectiveness is often called a resistance and the total resistance E^{-1} is said to be the sum of the resistances η^{-1}, η_f^{-1} due to pore and film diffusion respectively, a practice which equation (21) justifies in this case.

Conclusion

It has been shown that, if v_p/s_x is taken as the characteristic dimension of an irregularly shaped particle, the solutions of the steady state problem of simultaneous diffusion and reaction are largely independent of the particle shape. For the transient problem it will be shown in Part II that this characterisation is inadequate, and a new shape factor will be calculated.

Nomenclature

A = area of bed
a = radius of sphere or cylinder
C = concentration in fluid (or c_f)
c_s = surface concentration
D = diffusion coefficient of reactant in catalyst particle
D_f = diffusion coefficient of reactant in fluid
E = overall effectiveness factor
f_i = volume fraction of i^{th} size
h = film thickness
I_0, I_1 = modified Bessel functions
J_0, J_1 = Bessel functions
j_m = m^{th} root of $J_0(x) = 0$.
k = reaction rate constant
p = ratio radius : length of cylinder
R = region occupied by particle
S, S' = outer and inner surfaces of R
s_x = external surface area of particle
v_f = volume rate of fluid
v_p = particle volume
w_i = weight fraction
x = length coordinate
z = length coordinate
α' = voidage of bed
η = effectiveness factor
η_f = film effectiveness factor
$\lambda = (k\sigma/D)^{\frac{1}{2}}$
$\Lambda = v_p \lambda / s_x$
ρ = fraction of particle radius
σ = active catalyst surface/unit volume.
ϕ = shape factor
x = solution of (9)

References

[1] Amundson N. R. *Ind. Engng. Chem.* **48** 1956 26-42.

[2] Aris R. In preparation.

[3] Goldstein S. *Proc. Roy. Soc.* **A219** 1953 151-185.

[4] Hougen O. A. and Watson K. M. *Chemical Process Principles* Vol. III.

[5] Klinkenberg A. *Ind. Engng. Chem.* **46** 1954 2285-2289.

[6] Leva M. *Chem. Engng.* **56** 1949 115

[7] Lighthill M. J. and Whitham, G. B. *Proc. Roy. Soc.* **A229** 1955 281.

[8] Thiele E. W. *Ind. Engng. Chem.* **31** 1939 916.

[9] Wheeler A. *Advances in Catalysis* Vol. 2 (1951).

VOL
6
1956

Chemical Engineering Science, 1957, Vol. 6, pp. 269 to 276. Pergamon Press Ltd.

Studies in filtration

The initial stages of the cake filtration

P. M. Heertjes

Laboratory of Chemical Engineering of the Technical University Delft

(*First received* 11 *January* 1957; *in final form* 25 *February* 1957)

Abstract—The specific resistance of thin cakes has been investigated. This resistance (r) besides depending on the system is influenced by the initial filtration velocity and by the concentration (c) of the suspension, showing a decrease by increasing the velocity and the concentration.

An equation for the relation between r and c at constant initial filtration velocity has been given.

Résumé—L'auteur a étudié la résistance spécifique de gâteaux minces. Cette résistance (r) par ailleurs dépendant du système, est influencée par la vitesse de filtration initiale et par la concentration (c) de la suspension. Elle décroît quand la vitesse et la concentration augmentent.

L'auteur donne une équation pour la relation entre r et c à vitesse de filtration initiale constante.

VOL. 6 956/57

Introduction

It has been described in an earlier publication [1] that for the system puritine–nylon cloth the type of filtration is governed by the concentration of the suspension. Increasing the concentration (c) from a value of about 1 mg per litre showed first a blocking filtration [2] and than a cake filtration with a decreasing specific resistance of the cake (r) which resistance reached a constant low value. For the systems puritine–twillfill cloth and glass-spheres-nylon cloth no blocking filtration was found, but the influence of the concentration of the suspension on the cake resistance appeared to be the same as given above.

The main purpose of the work to be described here was to evaluate an equation for the relation between r and c and also to check for some other systems the validity of the observations made.

Experimental

(With R. de Boer, D. H. Jas and H. van Veen)

The experimental techniques and procedures used were the same as described in the two other papers [1, 2] to which the reader is referred. In a single case a small wooden plate and frame filterpress with three plates has also been used. A piston-pump transported the suspension in that case.

The suspensions were in water, the temperature was in all cases 20°C. For every experiment the normal precautions to prevent the filter effect were taken.

The substances used were: two types of puritine: Pur I [1] and Pur II (10-300 μ); a sieve fraction of Pur I: Pur I A (75-175 μ); Pur I A after dry elutriation for 1 hour: Pur I B; Pur I B after dry elutriation for another hour: Pur I C; the elutriation product obtained this way: Pur I D ($< 15\ \mu$); two sieve fractions of Pur II: Pur II A (75-175 μ) and Pur II B (175-300 μ); Norit (also an active carbon, containing $ZnCl_2$) and three sieve fractions: Norit A ($> 200\ \mu$, 27·5 per cent), Norit B (100-200 μ, 36·0 per cent) and Norit C (2-10 μ, 36·5 per cent); glass pearls as used before [1] (4-40 μ): Glass p.; sieved aluminium oxide (75-175 μ): Alum.

*In the puritine sieve fractions a rather large amount of particles much smaller than the smallest diameter of the sieves used occurred. These could be removed by elutriation with air.

Two different types of filtercloth have been used : nylon cloth (I) with 4000 openings per cm^2 and twillfill cloth (II) for which no reliable number of openings can be given. In the turbulent regime of flow the resistances (see below) were 0·56 and 2·0 respectively.

In the following the filters and cakes will be characterized by their resistance to flow (R_f for the filter, r for the cake (gram per cm^2) and R for cake + filter). As the conditions chosen for the filtration pressure and the resistance of the filter and the amount of cake were such that always turbulent flow existed†, the resistances R and R_f have been defined and calculated, by means of the equation :

$$\frac{1}{A}\frac{dV}{d\theta} = \frac{(\Delta P)^{0.55}}{R \text{ (or } R_f)} \qquad (1)$$

Moreover :

$$r = \frac{A}{c}, \frac{dR}{dV}. \qquad (2)$$

Therefore r has been calculated from the slope of the straight R-V line. The viscosity terms have been included in the resistance terms for convenience sake. This could be done because the experiments have been carried out at the same temperature of 20°C. Correction for the viscosity (η) can be made by dividing r and R_f by $\eta^{0.11}$. The pressure difference will be given in atmospheres (atm), length in cm and time in sec. Therefore R (or R_f) is expressed in :

$$\frac{(\text{atm})^{0.55}\,\text{sec}}{cm} \text{ and } r \text{ in } \frac{\text{atm}^{0.55}\,\text{cm sec}}{g}$$

RESULTS AND DISCUSSION

The results obtained and the discussion of these results will be presented in two paragraphs.

The influence of the initial filtration velocity on r

From earlier work indications were obtained that the cake resistance was not only influenced by the concentration of the suspension but also by the condition of the filtercloth. If this cloth was not cleaned thoroughly, no reproducible results could be obtained. Because the building up of the cake and therefore its resistance, for not too thick cakes, formed in not too long a time (with thick cakes other phenomena may occur such as a changed packing by continued flow or by diminuation of the flow velocity), is governed by the packing of the initial layers of the cake, a series of experiments have been carried out in which the resistance of rather thin layers of cake formed under different filtration conditions has been measured. Either the filtration pressure was changed and the cloth cleaned thoroughly before every experiment, or a series was carried out in which the cloth was only cleaned superficially by rinsing it in streaming tap-water after each experiment, thus increasing the cloth resistance because ever and anon some particles will remain in the cloth. In a few cases changes in ΔP and in R_f were combined. Some of the results are given in the Figs. 1, 2 and 3. In all cases r is presented as a function of the initial filtration velocity ;

$$U_0 = \frac{(\Delta P)^{0.55}}{R_f}$$

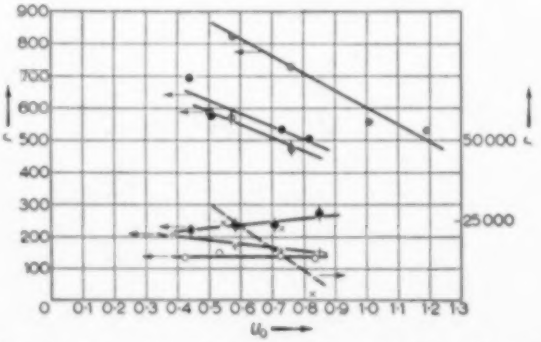

FIG. 1. The cake resistance r of Pur I and Pur II as a function of the initial filtration velocity U_0 for different concentrations.

Substance	Filter		Concentration.
×	Pur I	I	$1{\cdot}10^{-5}$
●	Pur I	I	$3{\cdot}10^{-5}$
⧫	Pur I	I	$5{\cdot}10^{-5}$
+	Pur I	I	$8{\cdot}10^{-5}$
○	Pur I	I	$10{\cdot}10^{-5}$
Φ	Pur II	I	$1{\cdot}10^{-5}$
⊕	Pur II	II	$1{\cdot}10^{-5}$

†It may be remarked that this also holds for the experiments of the first paper [1]. These have been calculated assuming laminar flow. The values given there should therefore be multiplied by $(0{\cdot}1)^{-0.45} = 2{\cdot}8$. The conclusions drawn there remain the same.

in which R_f is the resistance of the clean or incrustated filtercloth. It has been assumed that the relation between r and U_0 at a constant concentration can be expressed by :

$$r = \alpha + \beta U_0.$$

This relation has no physical basis at all and is used only to facilitate comparison. Straight lines based on this assumption, calculated by the method of the least squares have been drawn in the figures and evidently only give an approximative correlation and only between the limits of U_0 as measured. In Fig. 1 the results for Pur I and Pur II are presented ; here only the filtration pressure has been changed. In Fig. 2 the results for Norit and a mixture of 96 per cent Norit A and 4 per cent Norit C (weight basis) are presented ; here only R_f changed. In Fig. 3 the results for Pur I are given ; here both the filtration pressure and R_f have been altered. In Table 1 the calculated values of α and β have been assembled.

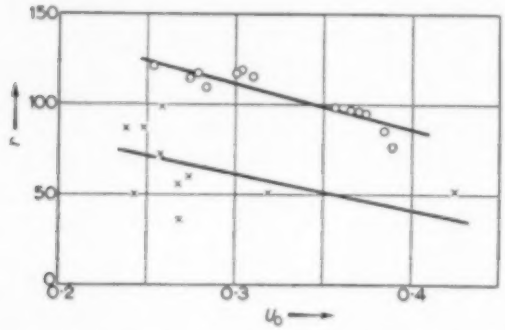

Fig. 2. The cake resistance r of Norit and of a mixture of Norit A and Norit C, as a function of the initial filtration velocity U_0.

○ = Norit
× = 96 per cent Norit A + 4 per cent Norit C

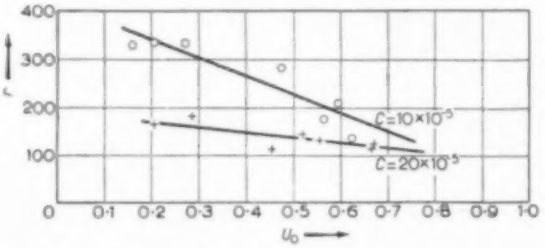

Fig. 3. The cake resistance r of Puritine I at two different concentrations as a function of the initial filtration velocity U_0.

Table 1

Substance	*Filter*	C	*Applied change*	α	β
Pur I	I	$10\cdot10^{-5}$	ΔP	140	− 14
		$8\cdot10^{-5}$	(range :	250	− 115
		$5\cdot10^{-5}$	0·07 → 0·25)	190	+ 100
		$3\cdot10^{-5}$		830	− 430
		$1\cdot10^{-5}$		65000	− 69000
Pur II	I	$1\cdot10^{-5}$		785	− 400
Pur II	II	$1\cdot10^{-5}$		1140	− 540
Norit	II	$10\cdot10^{-5}$		190	− 265
96 per cent Norit A + 4 per cent Norit C	II	$10\cdot10^{-5}$	R_f (range : 0·5 → 1·1)	120	− 200
Pur I	II	$10\cdot10^{-5}$	ΔP (range	415	− 380
		$20\cdot10^{-5}$	0·1 → 0·45) and R_f (range : 0·56 → 2·02)	190	− 110

Some experiments have been carried out in a filterpress with Pur I. It was not possible in this press to carry out a filtration at constant pressure. Therefore the press was operated under a more or less constant rate and the corresponding filtration pressure read. The variation in the pressure at each stroke of the pump was rather large, because no buffering zone was used. Again r has been plotted versus a U_0, which in this case has been taken as the velocity for the clean cloth corresponding to the filtration pressure measured. The constants calculated were :

$C = 5{\cdot}10^{-5}$	$\alpha = 195$	$\beta = +31$
$= 10{\cdot}10^{-5}$	$= 185$	$= +16$
$= 20{\cdot}10^{-5}$	$= 180$	$= +\ 3$
U_0^1 range	$= 0{\cdot}7 \rightarrow 2{\cdot}0$	
	$= 0{\cdot}5 \rightarrow 3{\cdot}0$	
	$= 1{\cdot}0 \rightarrow 6{\cdot}5$	

It is apparent that the accuracy of several experiments is not very great, especially of those at low concentrations and with the artificial mixture. This is not only caused by inaccuracies in the measurements, which are especially large at high values of r, but also by the experimental procedure, in which the apparatus has to be filled with water before the actual experiments start. This gives rise to a small volume region where the concentration changes, which may be accompanied by a rather big change in r in the beginning of the filtrations. The conclusions which can nevertheless be drawn from the data presented are that r depends on the initial filtration velocity, therefore on the velocity with which the particles arrive at the filter cloth. In general a cake formed at a low velocity compared with a cake formed at a high velocity, will show a denser packing and will therefore have a higher resistance, as found. An exception forms the experiment with Pur I over the nylon filter at a concentration of $5{\cdot}10^{-5}$, where the reverse is true. It is remarkable that using this concentration the experiments with Pur I always turned out to behave irregularly. An explanation has not been found.

A second conclusion is, that the influence of the filtration velocity on the cake resistance is more pronounced if the cake resistance is large, viz. if the packing of the cake is dense. Therefore for cakes formed from suspensions of a relatively high concentration the influence of the filtration velocity on the resistance of the cake is small and even can disappear.

The above is partly confirmed by the experiments in the filterpress with Pur I.

In analysing these results it has to be kept in mind that the first layers of the three cakes are formed at the lowest U_0 given and that the influence of U_0 as presented is not directly comparable with that of the experiments described before. Moreover whether the cakes are really compressible or whether the pulsating action of the pump caused a consolidation of the cake, cannot be decided here. However this parallelity with the former experiments exists : the influence of the increasing pressure difference – small in itself – diminishes with an increase of the concentration of the slurry from which the cakes are formed that is, diminishes with a decrease in the density of the packing.

The form of the r-c line

From paragraph (a) it follows that a reliable r-c relation can only be found under such conditions that always the same initial filtration velocity is guaranteed, which experimentally is most easily realized by using the same filtration pressure and a clean cloth. For nylon it was easy to clean the cloth, twillfill cloth was not so easy to clean causing greater uncertainty and greater deviations in the results. Precautions in this respect have always been taken as good as possible.

If by c_t is denoted the concentration at which the blocking filtration changes to the cake filtration, it has been found earlier for puritine that the resistance of the cake at this concentration (r_t) was about equal to the differential specific resistance of the blocking filtrations for $g = 0$. Therefore, including the results formed for blocking filtrations with puritine [2] :

$$r_t \sim (r_d)_{g \rightarrow 0} = \frac{R_f}{aN}\frac{S}{0}$$

Table 2. Filtration of Pur II over twillfill filtercloth at $\Delta P = 0{\cdot}21$ atm

No.	*Concentration (gram/litre)*	*r (atm.$^{0{\cdot}85}$ sec cm/g)*	*R_f (atm.$^{0{\cdot}85}$ sec/cm)*	*R'_f/R_f*
1	0·019	400	1·9	2·0
2	0·039	214	2·8	1·7
3	0·015	430	2·3	3·0
4	0·024	230	1·9	2·0
5	0·034	186	2·0	1·7
6	0·042	194	2·0	1·7
7	0·033	206	2·0	1·9
8	0·043	184	3·2	1·75
9	0·047	184	2·4	1·8
10	0·050	180	2·0	2·0
11	0·032	208	2·6	1·3
12	0·020	276	2·2	1·8
13	0·020	280	4·0	1·5
14	0·014	450	2·1	1·6
15	0·010	860	2·3	2·1
16	0·010	780	2·4	1·75
17	0·015	1260 → (1) →	1·2	7·0
18	0·024	640 → (2) →	1·2	7·0

From r_t onwards the resistance r decreases rapidly with an increase of the concentration to a rather low value, which upon further increase of the concentration remains constant, that is deviates not more than the experimental error from this value. The density of the packing of a cake, and therefore its resistance, at a certain filtration velocity, will depend on the amount of particles arriving per pore in the same time interval. Therefore r will depend on $\frac{c}{aN}$. For the type of relation between these two magnitudes a probability distribution seems likely, which will be given in the form :

$r - r_\infty = e^{-m\frac{c}{aN}}$, in which r_∞ is the value of the resistance at the concentration $c = \infty$. As $r = r_t$ for $c = c_t$, the relation can be changed to :

$$\frac{r - r_\infty}{r_t - r_\infty} = e^{-m\frac{c - c_t}{aN}} \qquad (3)$$

In equation (3) m is a proportionality constant which will depend on the pecularities of the system used. The $r - c$ relations obtained experimentally have been analysed with the aid of equation (3). Plotting r versus c and taking equal increments Δc, the corresponding r values can be used to find the magnitude of r_∞. The slope of the corresponding log $(r - r_\infty) - c$ line gives the value of $\frac{m}{aN}$.

It has been found that all the cases investigated can be represented by means of equation (3). Before giving the condensed results, as an example in Table 2 the $r - c$ data for the filtration of Pur II over twillfill cloth are tabulated and in Fig. 4 the $r - c$-line and the resulting log $(r - r_\infty) - c$ line are given. In Table 2 : $R'_f = R_{V\to 0}$. Large values of R'_f/R_f indicate that in these measurements the cloth has been clogged appreciably, giving too large values for r. The points indicated by (1) and (2) (see Fig. 4 and Table 2) have therefore not been used in drawing and using the $r - c$-line. In Table 3 the collected data are given. For the systems indicated by + no blocking filtration has been found. In these cases the value of $(r_d)_{c\to 0}$ and of $aN\frac{O}{S}$ could therefore not be evaluated. The value of r_t given here is the resistance of the cake at the lowest concentration c_t used. In case (11) the blocking filtration has not been measured and

Table 3

Substance	*Filter*	ΔP	$(r_d)_{g\to 0}$	$aN\frac{O}{S}$	c_t	r_t	r_∞	$\frac{m}{aN}$	$m\frac{O}{S}$
(1) Pur I	I	0·1	14000	$4\cdot10^{-5}$	$1\cdot10^{-5}$	11000	105	$3\cdot6\ 10^{4}$	1·4
(2) + Pur I	II	0·1	—	—	$1\cdot10^{-6}$	5600	140	$3\cdot3\ 10^{4}$	—
(3) + Glass p.	I	0·1	—	calc : $aN = 5\cdot2\cdot10^{-5}$	$3\cdot10^{-6}$	810	36	$3\cdot10^{4}$	1·6
(4) Pur I A	I	0·1	3640	$1\cdot5\ 10^{-4}$	$1\cdot10^{-4}$	3360	70	$1\cdot8\ 10^{4}$	2·7
(5) Pur I B	I	0·1	140	$4\cdot10^{-4}$	$2\cdot10^{-4}$	1260	140	$7\cdot0\ 10^{3}$	2·8
(6) Pur I C	I	0·1	28	$2\cdot10^{-2}$	$7\cdot10^{-4}$	—	—	—	—
(7) Pur I D	I	0·1	—	calc : $7\cdot10^{-5}$	$1\cdot10^{-5}$	7700	90	$4\cdot9\ 10^{4}$	3·4
(8) Pur II A	I	0·1	170	$3\cdot3\ 10^{-3}$	$2\cdot5\ 10^{-4}$	280	110	$2\cdot10^{4}$	66
(9) Pur II B	I	0·1	85	$6\cdot6\ 10^{-3}$	—	—	—	—	—
(10) + Pur II	II	0·16	—	—	$1\cdot10^{-5}$	825	180	$1\cdot7\ 10^{5}$	—
		0·21	—	—	$1\cdot10^{-5}$	770	185	$1\cdot8\ 10^{5}$	—
		0·40	—	—	$1\cdot10^{-5}$	560	185	$1\cdot3\ 10^{5}$	—
		0·50	—	—	$1\cdot10^{-5}$	535	170	$1\cdot0\ 10^{5}$	—
(11) Pur II	I	0·10	—	calc : $9\cdot6\ 10^{-4}$	$1\cdot10^{-5}$	585	220	$1\cdot0\ 10^{5}$	96
		0·16	—	$8\cdot0\ 10^{-4}$	$1\cdot10^{-5}$	570	230	$0\cdot9\ 10^{5}$	72
		0·22	—	$8\cdot3\ 10^{-4}$	$1\cdot10^{-5}$	475	240	$1\cdot0\ 10^{5}$	83
(12) Alum.	I	0·10	135	$4\cdot10^{-3}$	$7\cdot10^{-4}$	120	27	$1\cdot1\ 10^{3}$	4·4
(13) Alum.	I	0·10	200	$3\cdot10^{-3}$	$7\cdot10^{-4}$	—	—	—	—

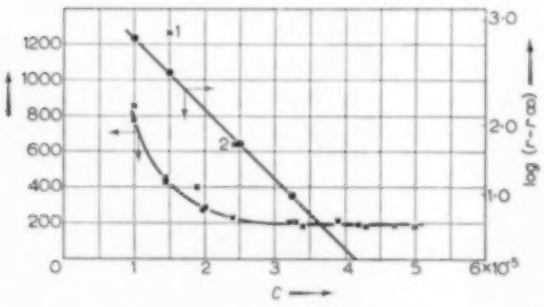

FIG. 4. The $r - c$ and $\log(r - r_\infty) - c$ relation for Puritine II filtered over twillfill cloth.

c_t and r_t here have the same significance as mentioned just before.

For the glass pearls the value of aN could be calculated from the size analysis of the product [1]. In the series (1) and (2) uncertainty existed over the value of r_t as measured. These values have not been included in the evaluation of $\frac{m}{aN}$. The r_t as given has been calculated with the aid of $\frac{m}{aN}$ found from the other points measured for the determined value of c_t given. The value of $m\frac{O}{S}$ has been calculated from $\frac{m}{aN}$ and $aN\frac{O}{S}$ by multiplication.

Finally some additional informations on Norit and its three sieve fractions are collected in Table 4, in which the values of r, determined at a filtration pressure of 0·1 atm and filtered over twillfill cloth are given.

Table 4

	$c = 10\cdot10^{-5}$	$c = 1\cdot10^{-5}$
Norit	128	871
Norit A	69	222
Norit B	55	417
Norit C	121	838
83·5 per cent A + 16·5 per cent C (weight basis)	107	566
92 per cent A + 8 per cent C (weight basis)	86	420

The following conclusions can be drawn. The relation between r and c is given by equation (3). The values of aN are such that at a not

VOL. 6 1956/57

very large concentration the value of r differs less than the experimental error from r_∞. As an example may be given that if the experimental error in r is assumed to be 1 per cent, for series (3) this concentration is at $10{\cdot}5\ 10^{-5}$, for series (7) at $8{\cdot}8\ 10^{-5}$. Therefore it is comprehensible that r rapidly reaches an apparently constant value; r_∞ can be taken for this value.

The value of $r_i \sim (r_d)_{g\to 0}$ as found earlier for one system. This fact is not surprising. For the systems investigated $\frac{O}{S}$ is constant (see later). Therefore $(r_d)_{g\to 0}$ is independent of the concentration. Increasing the concentration shows at c_i the gradual transition from blocking filtration to cake filtration. No abrupt change of the corresponding resistances can be expected of the very first layers of solid substance deposited. In agreement with paragraph (a), the value of r_∞ is independent of the filtration pressure, whereas at a lower concentration an influence of the pressure manifests itself in the influence of the initial filtration velocity, which governs the packing of the cake.

The parameter m introduced can not be calculated directly because $\frac{O}{S}$ is unknown. However in reasonable approximation for the cases investigated $\frac{O}{S}$ may be taken equal to unity,* in which case m can be read directly from Table 3. It can be concluded that m shows a great difference for Pur I and its fractions for which $m \sim 2$ and for the coarser Pur II and its fractions for which $m \sim 75$ filtered over nylon. It may be remarked that the values found for (11) may be too high, because they have been calculated with the aid of r_i as given which may be lower than the resistance at the transition point which has not been determined. The same holds for (7). A very great influence of the particle size spectrum and of the absolute size of the particles on the value of r_i is found. The influence on r_∞ is far less, if present at all.

The impression is gained that in the close packed cakes especially the smallest particles give a great increase of the resistance; compare (1) with (7) and with (4) and (5). This is not surprising. The denser a bed is packed, the larger will be the clogging effect by the smaller particles of the voids between the larger particles.

The strong influence of the small particles is again confirmed by the experiments with Norit and its three sieve fractions. A more systematic research on the influence of the size-spectrum on the cake resistance as well as on the significance of the parameter m is evidently necessary.

---

*In the publication on blocking filtration [2] it has been said that although in general $0 \neq S$, in the cases of substances having a rather wide size spectrum containing a large amount of relatively small particles, O was equal to S.

This conclusion was based on the fact that for these substances for different concentrations $\frac{OaN}{S}$ was found to be constant. The reasoning behind this was, that O and S change with the same variables but that in general O is also influenced by the form of the pores and of the particles. If however for one system the influence of the concentration is the same for S and O $\left(\frac{OaN}{S} \text{ is constant and therefore also } \frac{O}{S}\right)$ it seems likely that the extra influence of the form of the pores and the particles is not very large and therefore $0 \sim S$ in these cases. However for the sieve fractions investigated (Exp. 4, 5 and 8), the assumption that $\frac{O}{S} = 1$, seems far less justified, even if it is kept in mind that these fractions are far from monodispers. It had namely been found for the sieve fractions treated in the same paper that $\frac{OaN}{S}$ was not constant at different concentrations. However as has also been observed the values of S found for the lowest concentration used were always smaller than 1, which is a physical impossibility. All the values of S for these fractions can now be corrected by adding up a constant amount to each, such that not only $\frac{OaN}{S}$ becomes constant for each concentration, but also that each S is larger than 1. The calculated values of aN $\left(\frac{O}{S} \text{ taken equal to } 1\right)$, are given below.

The order of magnitude of these values is the same as those found by calculation with a mean value of a based on an apparent density of puritine of 1·0 and $N = 2250$. $60 - 90\ \mu$: $11{\cdot}10^{-5}$, $\frac{1}{2}(60 - 90\ \mu) + \frac{1}{2}(90 - 150\ \mu$: $15{\cdot}10^{-5}$, $90 - 150\ \mu$: $21{\cdot}10^{-5}$, $\frac{1}{2}(60 - 90\ \mu) + \frac{1}{2}(150 - 220\ \mu)$: $37{\cdot}10^{-5}$, $150 - 220\ \mu$: $27{\cdot}10^{-5}$.

CONCLUSION

For the systems investigated and for rather thin cakes it has been found that the resistance of the cake is determined, besides by the nature of the system, by the initial filtration velocity and by the concentration of the suspension. Both, by increasing give rise to a decrease of the specific resistance. For a constant initial velocity the relation between r and c can be given by the equation :

$$\frac{r - r_\infty}{r_i - r_\infty} = e^{-m\frac{c-c_i}{aN}}$$

in which r_i is the resistance at the concentration c_i and r_∞ is the asymptotic value of the resistance at an infinite concentration. The size and size spectrum have a large influence on the magnitude of r_i. The small particles determine the magnitude of r_i to a high degree. Many and relatively small particles increase the value of r_i.

NOMENCLATURE

A	= surface of the filter	cm^2
a	= weight of a particle	g
c	= concentration	gcm^{-3}
g	= amount of substance on the filter per cm^2	gcm^{-2}
m	= proportionality constant	cm
N	= number of pores of the filter per cm^2	cm^{-2}
O	= parameter	no dimension
ΔP	= filtration pressure	atm
R	= resistance per cm^2 filter surface of filter and cake	$atm^{0.55}$ sec cm^{-1}
r	= resistance of the cake per gram per cm^2 filter surface	$atm^{0.55}$ sec cm g^{-1}
R_f	= resistance of the filter per cm^2 filter-surface	$atm^{0.55}$ sec cm^{-1}
S	= parameter	no dimension
U_0	= initial filtration velocity	cm sec^{-1}
V	= volume of filtrate	cm^3
α	= $(r)_{U_0 \to 0}$	$atm^{0.55}$ sec cm g^{-1}
β	= parameter	$atm^{0.55}$ sec^2 g^{-1}

REFERENCES

[1] HEERTJES P. M. and VAN DER HAAS H. Studies in filtration. Part I. *Rec. Trav. Chim.* 1949 **68** 361.

[2] HEERTJES P. M. Blocking filtration, to be published in *Chem. Engng. Sci.*

Chemical Engineering Science, 1957, Vol 6, pp. 277 to 282. Pergamon Press Ltd.

A graphical method for the calculation of cooler-condensers

G. H. P. Bras

Chemical Construction Corporation, New York, U.S.A.

(*Received October* 1956)

Abstract—The method of Colburn and Hougen for the design of cooler-condensers is simplified by the use of a new graphical procedure for the determination of the liquid-gas interface conditions, by which trial and error computations are entirely eliminated.

The design method is based on the application of a diagram of the logarithm of the non-condensing gas partial pressure versus the temperature.

An example is given to illustrate the design method.

Résumé—L'auteur présente une simplification de la méthode de Colburn et Hougen pour le calcul des condenseurs réfrigérants, par utilisation d'une méthode graphique pour la détérmination des conditions à l'interface éliminant ainsi tout tatonnement et cause d'erreur.

La méthode graphique est basée sur représentation du logarithme de la pression particlle du gaz non condensable du mélange gaz-vapeur saturé en fonction de la température.

L'auteur donne un exemple pour illustrer cette méthode graphique.

VOL.
6
1956/57

The method of Colburn and Hougen [1] for the design of cooler-condensers for saturated gas-vapor mixtures requires the point to point solution of the equation,

$$h_0 (t_i - t_w) = h_g (t_g - t_i) + k_g \lambda_i (p_v - p_i) = U (t_g - t_w). \quad (1)$$

The heat transfer coefficient, h_0, is a combined coefficient for the cooling water side, the tube wall, scale and dirt deposits, and the film of condensate. It includes all heat resistances except those at the gas side, and it can easily be calculated by conventional methods. For most engineering calculations the combined heat transfer coefficient, h_0, varies little in the cooler-condenser, and can be taken as constant.

The gas-side heat and mass transfer coefficients h_g and k_g, can be calculated by any of the available correlations in the literature, e.g., by Chilton and Colburn's [2] equations,

$$h_g = \frac{j\, c\, G}{Pr^{\frac{2}{3}}} \quad (2)$$

$$k_g = \frac{j\, G\, M_v}{p_{gf}\, M_m\, Sc^{\frac{2}{3}}}. \quad (3)$$

If the inlet and outlet temperatures for the gas-vapor mixture and the cooling water are fixed, the intermediate values for the cooling water temperature, t_w, and the gas temperature, t_g, can be found from a simple heat balance in case of saturated gas-vapor mixtures, provided the gas-vapor mixture remains saturated during its flow through the cooler-condenser.

Inspection of the equations (1), (2) and (3) reveals that equation (1) contains two unknowns, namely the temperature and partial vapor pressure at the gas-liquid interface, t_i and p_i, while equation (3) contains one unknown, namely p_i, because $p_{gf} = (p_v - p_i)/\ln [(P - p_i)/(P - p_v)]$.

Colburn and Hougen [1] have therefore solved equation (1) by trial and error. After the calculation of various intermediate values of the total heat flux, $U (t_g - t_w)$, the tube area required can be calculated by graphical integration of the equation,

$$dQ = U (t_g - t_w)\, dA \quad (4)$$

or,

$$A = \int dA = \int \frac{d\, Q}{U (t_g - t_w)}. \quad (5)$$

Equation (1) neglects to account for the sensible heat of the diffusing vapors. A correction factor to take care of the sensible heat of the diffusing vapors was first proposed by Ackermann [3]. Based on this work, the author [4] has later derived equations for the apparent heat transfer coefficients at the gas side, and at the condensate side of the gas film, respectively. By the application of the correction factors involved, equation (1) can be more generally written,

$$h_0 (t_i - t_w) = h_g \cdot \frac{\epsilon\, e^{\epsilon}}{(e^{\epsilon} - 1)} \cdot (t_g - t_i) + k_g\, \Delta i\, (p_v - p_i) \quad (6)$$

or,

$$h_0 (t_i - t_w) = h_g \cdot \frac{\epsilon}{(e^{\epsilon} - 1)} \cdot (t_g - t_i) + k_g\, \lambda_i\, (p_v - p_i). \quad (7)$$

The numerical value of the correction factors in equations (6) and (7) is usually near to unity in most industrial cooler condensers. Thus, the correction factors may be neglected, except under extreme conditions. For the present purpose, it will be assumed that equation (1) is sufficiently accurate.

The trial and error calculations required for the solution of equation (1) are very time consuming. The author [5] has therefore proposed to solve this equation by a graphical procedure in a temperature-vapor pressure diagram.

Cairns [6] has proposed to express the relation between heat flux, $U\, \Delta\, t_{0v}$, and heat transferred, Q, by the equation for a parabola. This enables the calculation of the tube surface by analytical integration, if the heat flux is known for three values of Q. Cairns has obtained reliable results in four out of five cases. The author [7] has recently given another cooler condenser example, and the application of this design method also resulted in a relatively large deviation.

In the same article [7] a further simplification to the Colburn-Hougen design method was proposed. It was shown that the introduction of the group $F' = (L_v/C_m) \cdot (Pr/Sc)^{2/3}$, permits the elimination of the mass transfer coefficient, k_g. The factor F' has the dimension of a temperature differential. It varies but slightly for most gas-vapor mixtures over rather wide temperature ranges, so that it can often be taken as constant for design purposes.

In a later development of the graphical design method for cooler-condensers, the author [8] has shown that the graphical procedure can often be shortened by the application of a polar diagram. The polar diagram cannot be of much help when the combined heat transfer coefficient, h_0, shows great variations between inlet and outlet of the cooler-condenser, however.

There is thus room for further improvement in the design methods for cooler-condensers proposed so far. It is the purpose of this paper to present a new approach to the graphical determination of the gas-liquid interface conditions. This approach will eliminate all trial and error calculations and will deliver the interface conditions within the accuracy of the graphical procedure in a very simple way.

Design Equations

From equation 3 follows,

$$k_g = \frac{k_g'}{(p_v - p_i)} \cdot \ln \frac{(P - p_i)}{(P - p_v)} \quad (8)$$

where,

$$k_g' = \frac{j\, G\, M_v}{M_m\, Sc^{\frac{2}{3}}}. \quad (9)$$

If equation (8) is substituted in equation (1), the following relation is obtained after rearranging,

$$h_0 (t_i - t_w) = h_g (t_g - t_i) + k_g'\, \lambda_i \{\ln (P - p_i) - \ln (P - p_v)\} \quad (10)$$

or,

$$\frac{h_0}{h_g} (t_i - t_w) - t_g + t_i + \frac{k_g'\, \lambda_i}{h_g} \cdot \ln (P - p_v) = \frac{k_g'\, \lambda_i}{h_g} \cdot \ln (P - p_i) \quad (11)$$

From equations (2) and (9) follows,

$$\frac{k_g'\, \lambda_i}{h_g} = \frac{L_i}{C_m} \cdot \left(\frac{Pr}{Sc}\right)^{\frac{2}{3}} = F. \quad (12)$$

Substitution of $R = h_0/h_g$, and $F = k_g'\, \lambda_i/h_g$ in equation (11) delivers,

$$(R + 1)\, t_i - R\, t_w - t_g + F \ln (P - p_v) = F \ln (P - p_i) \quad (13)$$

Next, the temperature t_A will be defined,

$$t_A = \frac{R\,t_w + t_g - F \ln (P - p_v)}{(R + 1)} . \qquad (14)$$

Substitution of equation (14) in equation (13) gives after rearrangement,

$$\frac{(R + 1)}{F} \cdot (t_i - t_A) = \ln (P - p_i) . \qquad (15)$$

When no use is made of the simplification obtained by the introduction of the Factor $F = k_g' \lambda_i / h_g$, equation (15) will appear in the form,

$$\frac{(R + 1)\, h_g}{k_g' \lambda_i} . (t_i - t_A) = \ln (P - p_i) \qquad (16)$$

or,

$$\frac{(h_0 + h_g)}{k_g' \lambda_i} . (t_i - t_A) = \ln (P - p_i). \qquad (17)$$

The equations (15-17) still have the two unknowns t_i and p_i. However, the form of these equations enables the direct graphical determination of the gas-liquid interface temperature, t_i, by the following graphical procedure.

Graphical Procedure

In Fig. 1, a plot is shown of $\ln (P - p_s)$ against the temperature. First, this plot can be used for convenient computation of the value for $\ln (P - p_v)$ as required for the calculation of t_A, by equation (14).

Equation (15), can be brought in the following general form,

$$\frac{(R + 1)}{F} . (t - t_A) = \ln (P - p). \qquad (18)$$

Equation (18) represents a straight line in a diagram of $\ln (P - p)$ vs. t. The equation can be solved for two arbitrarily chosen values of t, e.g. t_D and t_E. This delivers two values of $\ln (P - p)$, namely $\ln (P - p)_D$ and $\ln (P - p)_E$, respectively. The points D and E can be plotted in Fig. 1. A straight line drawn through the points D and E in Fig. 1 will intersect the curve for $\ln (P - p_s)$ in point C. Point C will have the coordinates $\ln (P - p) = \ln (P - p_i)$, and $t = t_i$.

It can thus be seen that a direct solution of the interface temperature, t_i, is made possible by the use of a diagram of this type.

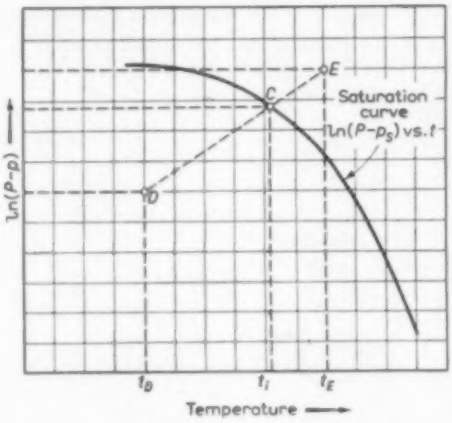

Fig. 1. Graphical determination of the interface conditions.

Evidently, this method will be accurate within the limits of the graphical computation. For engineering purposes it is usually accurate enough, if the temperature t_i can be taken from the diagram within 0·1 or 0·2°F.

Usually, it will be more convenient to bring equation (18) in the form,

$$\frac{(R + 1)}{2{\cdot}303\ F} . (t - t_A) = \log (P - p). \qquad (18a)$$

This equation enables to carry out the graphical procedure on commercially available semi-logarithmic graph paper, on which $(P - p_s)$ is plotted against the temperature.

Example

In order to check the accuracy of this graphical procedure, the method has been applied to the design of a cooler-condenser for a saturated mixture of carbon dioxide and water vapor. Complete design calculations for this condenser have been published elsewhere [7], and reference is made to this publication for all details.

The cooler condenser handles 7750 lb/hr of dry carbon dioxide, saturated with water vapor at 1 atm. and 203°F and cools it to 95°F. The cooling water enters at 77°F and leaves at 149°F, and flows in countercurrent with the gas stream. The cooler condenser is of the shell and tube type

Table 1. *Calculation of the reference temperature* t_A

Point No.	t_g °F	t_w °F	R	F' °F	$\frac{R+1}{F'}$	t_A °F
1	203·0	149·0	2·84	2,506	0·001531	− 167·6
2	202·1	141·75	2·98	2,510	0·001586	− 217·2
3	201·2	135·6	3·12	2,515	0·001642	− 260·0
4	199·4	126·05	3·39	2,516	0·001746	− 322·9
5	197·6	118·9	3·60	2,517	0·001830	− 373·5
6	194·0	108·9	4·01	2,538	0·001976	− 443·7
7	190·4	102·25	4·375	2,553	0·002106	− 487·7
8	185·0	95·7	4·86	2,569	0·002280	− 528·5
9	167·0	85·35	6·04	2,619	0·002687	− 581·4
10	149·0	81·15	6·775	2,669	0·002910	− 604·0
11	131·0	79·0	7·24	2,718	0·003030	− 618·7
12	113·0	77·75	7·59	2,767	0·003100	− 628·3
13	95·0	77·0	7·90	2,803	0·003175	− 628·8

and has 169 stainless steel tubes 1·05 inch O.D. and 0·824 inch I.D. on a triangular pitch. The gas flows at the shell side of the cooler condenser, and the cooling water flows inside of the tubes. The heat transfer coefficient, h_0, is equal to 71·8 B.t.u./hr sq. ft °F.

The calculation of the tube surface required for the condenser, requires the computation of the heat flux, $h_0 (t_i - t_w)$, at several intermediate points in the condenser and graphical integration of equation (5), where $U (t_g - t_w) = h_0 (t_i - t_w)$.

First, the cooling water temperature, t_w, is calculated for various intermediate temperatures of the gas-vapor mixture, t_g, by the application of a simple heat balance. If adiabatic conditions in the cooler-condenser are assumed, and the heat of the condensate is neglected, the following equation applies for counter-current flow,

Table 2. *Interface temperature and heat flux*

Point No.	t_i °F	$(t_i - t_w)$ °F	*Heat flux*		
			Via Graphical Procedure	*By Trial and error*	*Deviation*
			$h_0 (t_i - t_w)$ *B.t.u./hr sq. ft.*	$U (t_g - t_w)$ *B.t.u./hr sq. ft.*	%
1	202·4	53·4	3830	3830	0·0
2	201·4	59·65	4290	4270	+ 0·47
3	200·2	64·6	4645	4640	+ 0·11
4	198·0	71·95	5160	5150	+ 0·19
5	195·7	76·8	5510	5510	0·0
6	191·2	82·3	5905	5895	+ 0·17
7	186·3	84·05	6040	6025	+ 0·25
8	179·0	83·3	5980	5975	+ 0·08
9	153·8	68·45	4910	4925	− 0·30
10	130·5	49·35	3540	3540	0·0
11	110·3	31·3	2247	2275	− 1·23
12	95·5	17·75	1275	1263	+ 1·00
13	84·2	7·2	517	523	− 1·15

$G_0\,di_g = L\,c_w\,dt_w$. In this equation, i_g is the enthalpy of the saturated carbon dioxide-water vapor mixture, B.t.u./lb of vapour free gas.

Next, the heat transfer coefficient, h_g, is calculated from point to point by equation (2). Values for $R = h_0/h_g$ and $F' = (L_v/C_m)\cdot(Pr/Sc)^{\frac{1}{3}}$ are also calculated from point to point. Intermediate values for the reference temperature, t_A, can then be calculated by equation (14). In this example, the term $(P - p_v)$ in equation (14) has been multiplied by 10, in order to avoid negative numbers for the logarithms of small numbers. Accordingly, the graphical determination of the interface temperature, t_i, is carried out in a diagram of $\ln\left[10\,(P - p)\right]$ vs. the temperature, see Fig. 2.

The course of the calculations for the first point (gas entrance) is now as follows :

Gas temperature, $t_g = 203{\cdot}0°\text{F}$.

Cooling water temperature, $t_w = 149{\cdot}0°\text{F}$.

Partial water vapour pressure, $p_v = 0{\cdot}8341$ a.t.m.

Humidity, $\dfrac{0{\cdot}8341}{0{\cdot}1659} \times \dfrac{18}{44} = 2{\cdot}056$ lb/lb.

Total gas flow, $7750 \times 3{\cdot}056 = 23{,}650$lb/hr.

Maximum free area for gas flow at the baffled shell side, 1·755 sq. ft.

Gas Mass velocity, $\dfrac{23{,}650}{1{\cdot}755} = 13{,}500$ lb/hr sq. ft.

Viscosity of gas mixture, $\mu = 0{\cdot}0334$ lb/hr ft.

Heat capacity of gas mixture, $c = 0{\cdot}392$ B.t.u./lb °F.

Thermal conductivity, $k = 0{\cdot}01225$ B.t.u./hr ft °F.

Prandtl number, $Pr = c\,\mu/k = 1{\cdot}070$.

$Pr^{\frac{1}{3}} = 1{\cdot}047$.

Reynolds number $Re =$

$$\frac{1{\cdot}05 \times 13{,}500}{12 \times 0{\cdot}0334} = 35{,}300$$

Heat transfer factor, $j = 0{\cdot}0050$ (Reference [2], Fig. 2).

Heat transfer coefficient,

$$h_g = \frac{0{\cdot}0050 \times 0{\cdot}392 \times 13{,}500}{1{\cdot}047} = 25{\cdot}30 \text{ B.t.u./hr sq. ft. °F.}$$

$R = h_0/h_g = 71{\cdot}8/25{\cdot}30 = 2{\cdot}84$

$F' = (L_v/C_m)\cdot(Pr/Sc)^{\frac{1}{3}} = 2506°\text{F}$ (See reference [7]).

$\ln\left[10\,(P - p_v)\right] = \ln 1{\cdot}659 = 0{\cdot}5062$

Reference temperature,

$$t_A = \frac{(2{\cdot}84 \times 149) + 203 - (2506 \times 0{\cdot}5062)}{3{\cdot}84} = -167{\cdot}6°\text{F}.$$

Equation (18) gives, for $t_{D1} = 170°\text{F}$,

$$\ln\left[10\,(P - p)\right] = \frac{3{\cdot}84}{2506}\cdot(170 + 167{\cdot}6) = 0{\cdot}516\,;$$

for $t_{E1} = 220°\text{F}$,

$$\ln\left[10\,(P - p)\right] = \frac{3{\cdot}84}{2506}\cdot(220 + 167{\cdot}6) = 0{\cdot}593.$$

The two points D_1 and E_1 are plotted in Fig. 2, and a straight line drawn through D_1 and E_1 intersects the saturated curve in point C_1, representing the interface conditions. The interface temperature is read from the graph, or $t_i = 202{\cdot}4°\text{F}$. Heat flux, $h_0\,(t_i - t_w) = 71{\cdot}8\,(202{\cdot}4 - 149{\cdot}0) = 3830$ B.t.u./hr sq. ft.°F.

The calculations are repeated for the other intermediate points in the cooler-condenser.

In table 1, point to point values for t_g, R, F', $(R + 1)/F'$, and t_w are given as published previously [7]. The values for t_A shown in this table have been calculated as shown above.

In Fig. 2, the graphical determination of the interface conditions is shown (points $C_1 - C_{13}$). The abscissa of these points represent the interface

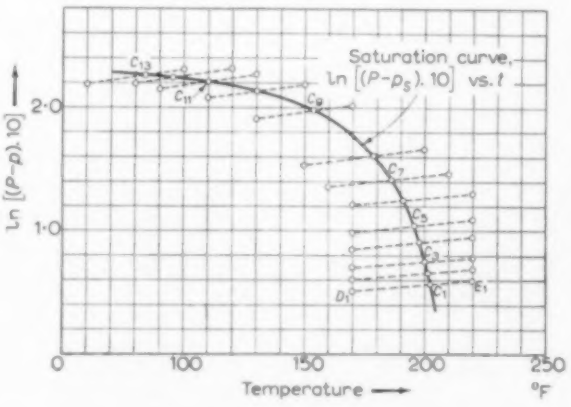

Fig. 2. Graphical solution of cooler condenser example.

temperature t_i. The values for t_i found graphically are listed in Table 2.

Table 2 also gives values for $(t_i - t_w)$ and the heat flux, $h_0\ (t_i - t_w)$. Further, point to point values of the heat flux calculated by trial and error are shown in this table as reported previously [7]. In the last column, the percent deviation between the two values is shown. The deviations are due to the graphical computation and they are well within the accuracy usually required for engineering calculations of this type.

Notations

A = Tube surface area, sq. ft.
c, c_{pv} = Specific heat at constant pressure of gas-vapor mixture and vapor, respectively, B.t.u./lb °F.
c_w = Specific heat of cooling liquid, B.t.u./lb°F.
C_m = Specific heat at constant pressure of gas vapor mixture, B.t.u./lb mole °F.
D = Diffusion coefficient, sq. ft/hr.
$F = k_g\, \lambda_i / h_g$, °F.
$F' = (L_v/C_m)\,.\,(Pr/Sc)^{\frac{1}{3}}$, °F.
G = Mass velocity of gas vapor mixture, lb/hr sq. ft.
G_0 = Flow rate of vapour-free gas, lb./hr.
h_0 = Combined heat transfer coefficient for cooling water, tube wall, scale, and condensate, B.t.u./hr sq. ft °F.
h_g = Gas film heat transfer coefficient, B.t.u./hr sq. ft °F.
Δi = Enthalpy difference between the vapor in the gas and the condensate on the tubes, B.t.u./lb. of vapor.
j = Heat and mass transfer factor, dimensionless.
k = Thermal conductivity of gas-vapor mixture, B.t.u./hr ft °F.
k_g = Gas film mass transfer coefficient, lb/hr. sq. ft. atm.
$k_g' = k_g\, p_{gf}$, lb/hr sq. ft.
L = Flow rate of cooling liquid, lb./hr.
L_i, L_v = Latent heat of condensation, respectively, at t_i, and at t_v B.t.u./lb mole.
M_v, M_m = Molecular weight of vapor and of gas-vapor mixture, respectively, lb/lb mole.
P = Total pressure, atm.
Pr = Prandtl number, $c\,\mu/k$, dimensionless.
p_s = Partial vapor pressure at saturation, atm.
p_v, p_i = Partial vapor pressure in the gas-vapor mixture, and at the gas-liquid interface, respectively, atm.
$\Delta p = p_v - p_i$, atm.
p_{gf} = Logarithmic mean partial pressure of non-condensing gas, atm.
Q = Total heat transferred, B.t.u./hr.
$R = h_0/h_g$, dimensionless.
Sc = Schmidt number, $\mu/\rho\, D$, dimensionless.
t = Temperature, °F.
t_A = Reference temperature, see equation 14, °F.
t_g, t_i, t_w = Temperature of gas mixture, of gas-liquid interface, and of cooling water, respectively, °F.
$\Delta t = t_g - t_i$, °F.
U = Overall heat transfer coefficient, B.t.u./hr sq. ft °F.
$\epsilon = -k_g\, \Delta p\, c_{pv}/h_g$.
$\epsilon = k_g\, \Delta p\, c_{pv}/h_g$, dimensionless.
λ_i, λ_v = Latent heat of condensation, respectively at t_i, and at t_v, B.t.u./lb.
ρ = Density of gas-vapor mixture, lb/cu. ft.
μ = Viscosity of gas-vapor mixture, lb/hr ft.

References

[1] Colburn A. P. and Hougen O. A. *Industr. Engng. Chem.* 1934 **26** 1178.
[2] Chilton T. H. and Colburn A. P. *Industr. Engng. Chem.* 1934 **26** 1183.
[3] Ackermann G. *Forsch. Ing. West., V.DI. Forschungsheft* 1937 No. 382.
[4] Bras G. H. P. *Chem. Engng.* 1954 **61** No. 12, 191.
[5] Bras G. H. P. *Chem. Engng.* 1954 **61** No. 5, 180.
[6] Cairns R. C. *Chem. Engng. Sci.* 1954 **3** 215.
[7] Bras G. H. P. *Petrol Refin.* 1936 **35** No. 6, 177.
[8] Bras G. H. P. *Petrol Refin.* 1957 **36** No. 2, 149.

Chemical Engineering Science, 1957, Vol 6, pp. 283 to 285 Pergamon Press Ltd.

Heat-transfer in cylindrical channels involving potential velocity distributions

SHIVA NANDAN SINGH

Department of Applied Mathematics
Indian Institute of Technology, Kharagpur, India

(*Received* 1 *October* 1956)

Abstract—Exact solution are presented for the problem of heat-transfer involving potential velocity distribution, in cylindrical channels, without making the usual assumption that $\frac{\partial^2 T}{\partial x^2} \ll \frac{\partial^2 T}{\partial r^2} + \frac{1}{r}\frac{\partial T}{\partial r}$. The temperature distribution is found to depend on the dimensionless parameters $\left[\frac{r}{s}, \frac{x}{s}, \frac{V_m x}{\alpha}, \frac{As^2}{\alpha}\right]$ and not on $\left[\frac{r}{s}, \frac{\alpha}{sV_m}\cdot\frac{x}{s}, \frac{As^2}{\alpha}\right]$ as in the approximate treatment of the problem.

Résumé—Les auteurs presèntent des solutions exactes du transfert de chaleur avec distribitution de vitesses, dans les canaux cylindriques sans faire l'hypothèse habituellè :

$$\frac{\partial^2 T}{\partial x^2} \ll \frac{\partial^2 T}{\partial r^2} \pm \frac{1}{r}\frac{\partial T}{\partial r}$$

Ils trouvant que la distribution de la température dépend des paramètres sons dimensions :

$$\frac{r}{s}, \frac{x}{s}, \frac{Vmx}{\alpha} \frac{As^2}{\alpha} \text{ et non de } \frac{r}{s}, \frac{\alpha}{sVm}\cdot\frac{x}{s}, \frac{As^2}{\alpha}$$

Comme dans le calcul approximatif du problème.

1. INTRODUCTION

TOPPER [1] investigated the temperature distribution for plug flow, in cylindrical channels, kept at constant wall temperature, with uniform and constant generation of heat within the fluid, when the fluid enters the channel at a prescribed temperature. He also considered the problem of temperature equalization, when the inlet temperature has one constant value for part of the radius, and another value for the rest of the radius. The solution of the first problem is helpful in estimating temperatures developed in chemical and nuclear reactors, and that of the second problem in estimating average life of non-uniformities of the temperature in such streams.

His treatment of these problems is approximate and is based on the assumption that $\frac{\partial^2 T}{\partial x^2} \ll \frac{\partial^2 T}{\partial r^2} + \frac{1}{r}\frac{\partial T}{\partial r}$. The solution of the simplified energy equation reveals that the temperature distribution depends only on non-dimensional quantities $(r/s, As^2/\alpha)$ and a dimensionless group $\left(\frac{\alpha}{s\,V_m}\cdot\frac{x}{s}\right)$.

In this paper, we give exact solution of the energy equation corresponding to TOPPER's problem. We find that the temperature distribution depends on the dimensionless quantities $\left[\frac{r}{s}, \frac{x}{s}, \frac{V_m x}{\alpha}, \frac{As^2}{\alpha}\right]$. The dimensionless group $\left(\frac{\alpha}{s\,V_m}\cdot\frac{x}{s}\right)$ does not appear in the exact solution.

2. UNIFORM HEAT GENERATION

Consider a stream of fluid entering the channel of radius $r = s$. At $x = 0$, the stream temperature is T_0, and the uniform wall temperature is T_s. The energy equation for steady state, and in case of axial symmetry simplifies as

$$V_x \frac{\partial T}{\partial x} = \alpha \left(\frac{\partial^2 T}{\partial r^2} + \frac{1}{r} \frac{\partial T}{\partial r} + \frac{\partial^2 T}{\partial x^2} \right) + q\rho/c. \quad (1)$$

θ is defined by the relation

$$T = \theta e^{-\lambda x} + T_s, \quad (2)$$

with the boundary conditions

$$\theta = 0, \text{ for } x > 0 \text{ and } r = s. \quad (3)$$

$$\theta = \theta_0 = T_0 - T_s, \text{ for } x = 0 \text{ and } r < s. \quad (4)$$

In case of potential flow, V_x is constant V_m, and (1) becomes

$$\frac{\partial^2 \theta}{\partial r^2} + \frac{1}{r} \frac{\partial \theta}{\partial r} + \frac{\partial^2 \theta}{\partial x^2} - \lambda^2 \theta = - \frac{A e^{\lambda x}}{\alpha} \quad (5)$$

$$\text{where } \lambda = - (V_m/2\alpha). \quad (6)$$

The complete solution of equation (5) is

$$\theta = \sum_{n=1}^{\infty} B_n e^{-\sqrt{\beta_n^2 \left(\frac{r}{s}\right)^2 + \lambda^2 x^2}} \cdot J_0 \left(\beta_n \frac{r}{s} \right) + \frac{A s^2 e^{\lambda x}}{4 \alpha} \left(1 - \frac{r^2}{s^2} \right) \quad (7)$$

where B_n and β_n are constants. J_0 is the Bessel function of the first kind and of zero order. The condition (3) is satisfied if β_n are zeros of $J_0 (\beta_n)$, and (4) gives

$$\theta_0 = \sum_{n=1}^{\infty} B_n J_0 (\beta_n w) + \frac{A s^2}{4 \alpha} (1 - w^2) \quad (8)$$

where $w = (r/s)$.

Multiplying (8) by $J_0 (\beta_m w)\, w\, dw$, where β_m need not be the same eigen value as β_n, and integrating within the limits zero to 1, we have for each n,

$$B_n = \frac{2 \theta_0}{\beta_n J_1 (\beta_n)} \left[1 - \frac{A s^2}{\alpha \theta_0} \frac{1}{\beta_n^2} \right]. \quad (9)$$

Finally

$$\frac{T - T_s}{T_0 - T_s} = \sum_{n=1}^{\infty} \left. \begin{aligned} & \frac{2 e^{-\lambda x}}{\beta_n J_1 (\beta_n)} \left(1 - \frac{A s^2}{\alpha \theta_0} \cdot \frac{1}{\beta_n^2} \right) \\ & e^{-\sqrt{\beta_n^2 \left(\frac{r}{s}\right)^2 + \lambda^2 x^2}} \cdot J_0 \left(\beta_n \frac{r}{s} \right) \\ & + \frac{A s^2}{4 \alpha \theta_0} \left(1 - \frac{r^2}{s^2} \right) \end{aligned} \right\} \quad (10)$$

3. Temperature Mixing Between Concentric Streams

In this case, the temperature of the entering fluid (at $x = 0$) is assumed to be T_a for part of the radius, say from $r = o$ to $r = a$, and T_b for the rest of the radius (from $r = a$ to $r = s$). The wall temperature remains constant T_s. The energy equation (1) with $q = 0$ simplifies to

$$\frac{\partial^2 \theta}{\partial r^2} + \frac{1}{r} \frac{\partial \theta}{\partial r} + \frac{\partial^2 \theta}{\partial x^2} - \lambda^2 \theta = 0, \quad (11)$$

where $T = e^{-\lambda x} \theta + T_s$.

The boundary conditions are

$$\text{at } x = 0, \ \theta = \theta_a = T_a - T_s, \ a > r > 0, \quad (12)$$

$$\theta = \theta_b = T_b - T_s, \ s > r > a,$$

$$\text{at } r = s, \ \theta = 0. \quad (13)$$

The solution is

$$\theta = \sum_{n=1}^{\infty} B_n e^{-\sqrt{\beta_n^2 \left(\frac{r}{s}\right)^2 + \lambda^2 x^2}} \cdot J_0 \left(\beta_n \frac{r}{s} \right). \quad (14)$$

where β_n are the positive roots of $J_0 (\beta_n) = 0$. B_n are determined from (12).

$$B_n \int_0^1 J_0 (\beta_n w)\, J_0 (\beta_m w)\, w \, . \, dw = \theta_a \int_0^{a/s} J_0 (\beta_m w)\, w dw + \theta_b \int_{a/s}^1 J_0 (\beta_m w)\, w dw. \quad (15)$$

Hence $$B_n = \frac{2}{\beta_n \{J_1 (\beta_n)\}^2} \left[\frac{a}{s} (\theta_a - \theta_b) J_1 \left(\beta_n \frac{a}{s} \right) + \theta_b J_1 (\beta_n) \right]. \quad (16)$$

And finally

$$\frac{T - T_s}{T_b - T_s} = \sum_{n=1}^{\infty} \left. \begin{aligned} & \frac{2 e^{-\lambda x}}{\beta_n \{J_1 (\beta_n)\}^2} \\ & \left[\frac{a}{s} \frac{T_a - T_b}{T_b - T_s} J_1 \left(\beta_n \frac{a}{s} \right) \right. \\ & \left. + J_1 (\beta_n) \right] e^{-\sqrt{\beta_n^2 \left(\frac{r}{s}\right)^2 + \lambda^2 x^2}} \cdot J_0 \left(\beta_n \frac{r}{s} \right). \end{aligned} \right\} \quad (17)$$

4. Discussion of the Results

From equations (10) and (17), it is obvious that the temperature of the fluid at any point is a function of $\left[\frac{r}{s}, \frac{x}{s}, \frac{V_m x}{\alpha}, \frac{A s^2}{\alpha}\right]$ whereas in Topper's example, the temperature depends on $\left(\frac{r}{s}, \frac{\alpha}{s V_m} \cdot \frac{x}{s}, \frac{A s^2}{\alpha}\right]$. He plots the temperature distribution on the axis of the channel ($r = 0$), against the abscissa $\left(\frac{\alpha}{S V_m} \cdot \frac{x}{s}\right)$. Here it is not possible to compare the results with those of Topper's, because the temperature cannot be plotted as a function of $\left(\frac{\alpha}{S V_m} \cdot \frac{x}{s}\right)$.

4. Notations

$A = (q/\rho c)$, uniform heat generation.
J_0, J_1 = Bessel function of the first kind, and of zero and first order.
B_n = coefficient of characteristic function in various equations.
T, T_a, T_b, T_0, T_s = temperature, initial temperature at $r < a$, initial temperature at $a < r < s$, initial temperature, wall temperature.
V_m, V_x = mean velocity, local axial velocity.
a = radial coordinate at discontinuity of initial temperature.
c = heat capacity.
q = heat generation per unit volume and time.
r = radial coordinate.
s = tube radius.
$w = (r/s)$.
x = axial coordinate.
α = thermal diffusivity.
β_n = a zero of J_0.
ρ = density.
θ_0, θ at $w = 0$, and $\theta = (T - T_s)\, e^{\lambda x}$.
$\lambda = -(V_m/2\alpha)$.

In conclusion, I thank Dr. S. D. Nigam for suggesting this problem to me.

Reference

[1] Topper Leonard *Chem. Engng. Sci.* 1956 **5** 1 13-19.

VOL. 6 1956/57

Book reviews

VICTOR GOLD: **pH Measurements.** Methuen Monograph, 1956. 125 pp. 9s. 6d.

THERE is a story of a Professor who remarked, on reading a student's doctoral thesis, "There is much that is true and much that is new in this thesis, but that which is true is not new, and worse, that which is new is not true." Dr. GOLD, in his Methuen Monograph on pH measurements, has tried hard to avoid the second fault, and has succeeded completely in keeping to established theoretical and experimental results.

Where, however, there is less certainty about the measuring of pH, as for example near detergent micelles, polyelectrolyte molecules or charged surfaces, Dr. GOLD offers no suggestions, preferring to remain on the solid ground of long established fact rather than venture into the quicksands of contemporary research.

An author's approach, however, is always a matter of taste, and the book must also be judged on the material therein as well as on its general scope. There is no doubt that Dr. GOLD has been meticulously painstaking in selecting his pH standards and in discussing how they should be used. The book is thus of interest to anyone working on very accurate pH measurements (i.e. to better than 0·01 pH unit) and to those interested in the physical meaning of pH determinations.

In the reviewer's opinion, however, this is a book on pH which virtually ends the fundamental importance of the pH scale: now that there are very fundamental difficulties in reconciling the different definitions and measurements of pH (i.e. pcH, pH, pwH, psH), might not anyone working outside the field of acid-base catalysis prefer to quote the result of a measurement with some standard pH meter and leave it at that?

Where a fuller discussion might have been useful is in the field of non-aqueous solvents. The recent importance of titrating long-chain acids and polymers in non-aqueous solvents would seem to have justified this.

Finally, who is the book intended for? The research physical chemist would probably turn up the fourth edition of Britton's book "Hydrogen Ions," (1956), or BATES' book "Electrometric pH Determinations" (1952). The chemical engineer would, like the reviewer, probably be content to read the instructions on the pH meter. However, the industrial research chemist who requires a ready guide to pH determinations, who requires considerable accuracy or who wants to measure a pH which has some reasonable physical interpretation, will find this little book a clear, useful and accurate bench companion.

J. T. DAVIES

Physical Methods in Chemical Analysis. Vol. III. Edited by W. G. BERL, Academic Books Ltd., London, 1956. xii + 652 pp. $15.00.

TO AN increasing extent the science of chemistry is being facilitated by the development and availability of physical methods for qualitative and quantitative analysis in the widest sense of the word. Books concerned with these newer specialized methods are becoming more prevalent; in essence they must provide reasonably comprehensive, clearly-written reviews that are understandable to the non-expert. In general, BERL's Volume III maintains the high standard of the earlier volumes, and some of its 12 chapters are excellent. In others the Reviewer feels that the space allotted has been too small so that, although the theory and general principles are stressed, and rightly so, the number of actual examples of the scope and uses of the particular technique is too small. A book of the same length covering 6–9 of the topics would probably be of more value to the chemist, chemical engineer, or analyst. Two of the topics discussed – gas chromatography and nuclear magnetic resonance spectroscopy – are of particular current interest. It is only a few years since the potentialities of these techniques were realized, but today relatively inexpensive gas chromatography instruments and distinctly expensive, but none-the-less highly useful, nuclear magnetic resonance spectroscopy instruments are available commercially. The chapter on gas chromatography, written by a pioneer of the technique, provides an excellent introduction to the subject, but is disappointingly short (27 pp.) compared with many of the other chapters. Thus the reader must seek elsewhere for more detailed information, and, although the list of 35 references includes most of importance up to 1955, one wishes that it were more comprehensive. The section on nuclear magnetic resonance spectroscopy is longer, with an adequate reference list. Written by a leader in the field, it constitutes one of the best reviews yet available and covers theory, experimental methods, and the interpretation and uses of this important branch of spectroscopy. The uses of neutron spectroscopy in chemical analysis are admirably summarized, often in tabular form, in the longest and most comprehensive chapter of the book. Electrochromatography is another relatively new technique and its practical applications, particularly in the biochemical field, are emphasized in a review that sets forth the principles and describes in some detail the apparatus required; the diagrams in this chapter are particularly good. Other topics covered are electroanalytical methods in trace analysis, the high frequency method of analysis, field emission spectroscopy, flame photometry, microwave spectroscopy, fluorescent X-ray spectrometric analysis, and analytical distillation; a section on

the theory and principles of sampling for chemical analysis is a useful addition.

The book is well printed and reasonably free from errors. Despite the high price that one has come to expect for a compendium of this type, this is a recommended book with which all practising chemists and chemical engineers should be familiar.

R. N. HASZELDINE

McCABE and SMITH: **Unit Operations of Chemical Engineering.** McGraw-Hill, New York, 1956. 956 pp. 79s.

THIS book has been written for students who are meeting unit operations for the first time. It assumes only a knowledge of elementary mathematics and physics. In common with previous books on the same subject, a broad interpretation is taken of the scope of unit operations. Over a quarter of the book is devoted to fluid mechanics and heat transfer. An excellent introduction is given to fluid friction and boundary layer theory. The importance and applications of dimensional analysis are stressed throughout the book.

All of the unit operations normally covered in a University course are discussed. Multicomponent separations, transient phenomena, and operations at extremes of temperature, pressure, or velocity have been deliberately omitted. Some discussion of these points would be desirable, particularly since these fields are becoming increasingly important.

The chief criticism that can be offered is that the book is too long, and, as a consequence, too expensive. Books intended for undergraduate use should be carefully pruned of all material not absolutely essential if they are to be of the greatest value. This might be done by eliminating the long introduction (which is essentially an introduction to chemical engineering), and by reducing the large amount of space given to description of equipment. For example, twenty-three pages are used to describe pipe, pipe fittings, and valves. The descriptions of equipment are, in fact, excellent, but a separate book might be a better place for most of them.

Professors McCABE and SMITH have, however, produced a very readable book which deserves a place on the chemical engineering bookshelf.

G. A. RATCLIFF

VOL.
6
956/57

SOME CURRENT PAPERS IN OTHER JOURNALS

Chemical Engineering Progress

VOLUME 53, No. 4 (partial contents) APRIL 1957

A. Charnes and W. W. Cooper: Linear programming—solving management problems 170

A. C. Dreshfield, Jr.: Mechanism of hot surface drying of fibrous sheets 174

F. G. Kerry: Safety aspects of air separation plant cycles 181

E. C. Clark (Edited by): Discussion of air separation plant safety 185

E. Karwat: Linde's view on air separation plant safety 188

W. E. Katz: Status of electric membrane demineralization 190

J. A. A. Greathead and W. H. C. Simmonds: Mixing patterns in helical-flight mixers .. 194

N. M. Levitz, E. J. Petkus, H. M. Katz, and A. A. Jonke: Fluidized bed process produces UF_4 199

P. A. Haas, E. O. Nurmi, M. E. Whatley, and J. R. Engel: Midget hydroclones remove micron particles 203

VOL 6 1956

ERRATUM

Houghton G., McLean A. M., and Ritchie P. D. Compressibility, fugacity, and water solubility of carbon dioxide in the region 0-36 atm and 0-100°. *Chem. Engng. Sci.* 1957 **6** 132.

The first line of equation (3) in the left-hand column of page 133 should read :

$$Z = \frac{PV}{RT} = 1 + \frac{P}{RT}$$

VOL.
6
956/57

END